DOI: 10.1002/ejic.200800513

Soft–Soft Interactions Involving Iodoselenophosphonium Cations: Supramolecular Structures of Iodine Adducts of Bulky Trialkylphosphane Selenides

Wolf-W. du Mont,*[a] Michael Bätcher,[a] Constantin Daniliuc,[a] Francesco A. Devillanova,[b] Christian Druckenbrodt,[a] Jörg Jeske,[a] Peter G. Jones,*[a] Vito Lippolis,[b] Frank Ruthe,[a] and Emma Seppälä[a]

Keywords: Phosphane selenides / Iodine / Soft–soft interactions / Supramolecular structures / X-ray crystallography / FT-Raman spectroscopy

The reactions of trialkylphosphane selenides $t\mathrm{Bu}_n i\mathrm{Pr}_{3-n}\mathrm{PSe}$ (n = 3: **1a**; n = 2: **1b**; n = 1: **1c**; n = 0: **1d**) with iodine are studied with the help of heteronuclear NMR spectroscopy, vibrational spectroscopy, and X-ray crystal structure determinations. The reaction of **1a** with one equivalent of iodine provides, after crystallization from dichloromethane/pentane, solid **2a**, which consists of pairs of molecular adducts $t\mathrm{Bu_3PSe{-}I{-}I}$, together with chains of alternating $[(t\mathrm{Bu_3PSe})_2\mathrm{I}]^+$ and $\mathrm{I_3}^-$ ions. The addition of iodine to **1b**, **1c**, and **1d** in a 1:1 molar ratio furnishes ionic solids with the formulation $[(t\mathrm{Bu}_n i\mathrm{Pr}_{3-n}\mathrm{PSe})_2\mathrm{I}]^+[\mathrm{I_3}]^-$ (n = 2: **2b**; n = 1: **2c**; n = 0: **2d**). Compounds **2a**–**2d** exhibit supramolecular structures based on various kinds of weak Se···I and Se···Se interactions. In **2a**, the uncharged molecules form dimers through Se···Se contacts, while the anions and cations assemble to form chains through linear $\mathrm{P{-}Se{\cdots}I_{anion}}$ contacts. The ionic compounds **2b** and **2d** consist of the same type of chains, although they are not isotypic to each other. The two independent formula units of **2c** are topologically different; one forms cation–anion chains analogous to those of **2b** and **2d**, whereas the other forms cation chains through Se···Se contacts. Se···I contacts between the latter chains and triiodide anions are very long but seem to be structurally significant; for such contacts, at well above the sum of the van der Waals radii, we propose the term *tertiary contacts*. On using more than one equivalent of $\mathrm{I_2}$, compounds corresponding to the formulation $t\mathrm{Bu}_n i\mathrm{Pr}_{3-n}\mathrm{PSeI}_x$ (x = 3, n = 3: **3a**; x = 4, n = 1: **4c**; x = 7, n = 2 and 0: **5b** and **5d**) were isolated as single crystals. Ionic **3a** contains pairs of cations $[(t\mathrm{Bu_3PSe})_2\mathrm{I}]^+$, connected by Se···Se contacts, located between corrugated layers of polymeric $\mathrm{I_5}^-$ anions. Compound **4c** consists of two independent formula units $t\mathrm{Bu}i\mathrm{Pr_2PSeI_2{\cdot}I_2}$, which could, however, be regarded as $t\mathrm{Bu}i\mathrm{Pr_2PSeI^+{\cdot}I^-{\cdot}I_2}$ because of the long I–I distance adjacent to Se. To a fair approximation, the packing of the two units is independent; unit 1 forms dimers $(\cdots\mathrm{Se{-}I{-}I}\cdots\mathrm{I{-}I}\cdots)_2$, whereas the same motif in unit 2 forms chains. The structural subunits are linked through further contacts involving terminal iodine atoms from $t\mathrm{Bu}i\mathrm{Pr_2PSeI}\cdots\mathrm{I}$ units, which thereby form μ_3-bridging units, and by additional I–I···Se contacts. In **5b**, iodide-bridged cations $[t\mathrm{Bu_2}i\mathrm{PrPSeI}\cdots\mathrm{I}\cdots\mathrm{ISeP}i\mathrm{Pr}t\mathrm{Bu_2}]^+$ are anchored to a polyiodide network of formal composition $\mathrm{I_{11}}^-$ [= $(\mathrm{I^-})(\mathrm{I_2})_5$] through I···I contacts. Except for one I···I contact, the polyiodide is two-dimensional, although highly puckered. In **5d**, $[i\mathrm{Pr_3PSeI}]^+$ cations and $\mathrm{I_2}$ molecules exhibit weak I···I interactions with $\mathrm{I^-}$ units from puckered square-net-like polyiodide layers.
(© Wiley-VCH Verlag GmbH & Co. KGaA, 69451 Weinheim, Germany, 2008)

Introduction

Phosphane sulfides, selenides, and tellurides are known to act as donors towards dihalogen molecules.[1–8] Two types of molecular 1:1 adducts $\mathrm{R_3PEX_2}$ are well established: compounds that feature either approximately linear E–X–X arrays (E = S, Se, and X = I) having a *two*-coordinated central I atom (10-I-2),[9] type **A** (Scheme 1), or compounds featuring T-shaped $\mathrm{PEX_2}$ cores (E = Se and X = Br,[8,10,11] or E = Te, and X = Cl, Br, I) having a *three*-coordinated central E atom (10-E-3), type **B** (Scheme 1).[12] Type **A** complexes exhibit X–X bond orders (<1) that correlate negatively with the donor properties of $\mathrm{R_3PE}$: strong n(E)→σ*(X–X) donation leads also to increasing E–X interactions and decreasing P–E bond orders.[13] Type **B** complexes contain "ylidic" P–E single bonds and 3c–4e X–E–X systems[7–9,12] the latter are related to those in "hypervalent" (10-E-3) $\mathrm{RTeI_2}^-$ anions.[14] Among 1:1 iodine adducts of phosphane sulfides and selenides, type **A** structures are abundant, and solid polyiodine adducts $(\mathrm{Ph_3PS})_x(\mathrm{I_2})_y$ (x/y = 2:3 or 1:3) are also best described as molecular complexes

---

[a] Institut für Anorganische und Analytische Chemie der Technischen Universität Braunschweig,
Postfach 3329, 38023 Braunschweig, Germany
Fax: +49-531-3915387
E-mail: w.du-mont@tu-bs.de
[b] Dipartimento di Chimica Inorganica ed Analitica, Complesso Universitario di Monserrato,
S.S. 554 Bivio per Sestu, 09042 Monserrato (CA), Italy
Fax: +39-0706754456
E-mail: devilla@unica.it

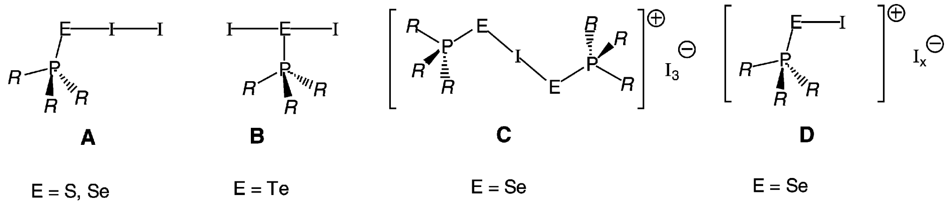

Scheme 1. Various types of iodine adducts of phosphane chalcogenides.

(type **A** with additional $I_2\cdots I_2$ interactions),[2] whereas Et_3PTeI_2 represents the only R_3PEX_2 adduct of type **B** with E = Te and X = I (Scheme 1).[12]

Our first experiments in this field provided the solid 1:1 adduct tBu$_3$PSeI$_2$ (**2a**) as product from the reaction of tBu$_3$PSe (**1a**) with iodine;[6,7] it turned out to contain, in the same crystal, both type **A** molecular adducts and chains from weakly interacting $[(t\text{Bu}_3\text{PSe})_2\text{I}]^+$ (type **C**) cations and I_3^- anions. On using a slight excess of iodine, solid ionic $[(t\text{Bu}_3\text{PSe})_2\text{I}]^+[\text{I}_5]^-$ (**3a**) was isolated.[15]

tBu$_3$P is an exceptionally bulky ligand and the question arose whether this property promoted the energetic equivalence of the ionic and the molecular structure in **2a**. This led us to evaluate the roles of substituents on the nature of solid halogen adducts of trialkylphosphane selenides. Since triarylphosphane selenides (weaker donors than **1a**) and tris(dialkylamino)phosphane selenides (stronger donors than **1a**) both gave type **A** adducts,[5] while tBu$_2$P(I)=Se with iodine led to a *soft–soft base pair* through dimerization of a special type **A** adduct (with an iodine substituent at phosphorus),[6,7] we found it desirable to *tune* the steric bulk in trialkylphosphane selenides related to **1a** and to vary the reaction conditions, in order to establish whether bulky **1a** was unique in leading to type **C** structures. Husebye et al. had detected that on iodination of two aminophosphane selenides, polyiodide formation led to generation of $[R_3P–Se–I]^+$ cations (type **D**) that are – in the solid state – in close contact with triiodide and tetraiodide networks.[4] In a preliminary report, structures of two type **D** hexaiodide salts were reported,[15] and a recent study of the bromine addition to trialkylphosphane selenides $t\text{Bu}_n i\text{Pr}_{3-n}\text{PSe}$ (n = 3: **1a**; n = 2: **1b**; n = 1: **1c**; n = 0: **1d**) revealed that each of the closely related (10-Se-3) compounds, including two modifications of iPr$_3$PSeBr$_2$, exhibit, in a remarkable fashion, their particular patterns of intermolecular soft–soft interactions.[11] In the following, we present a study on supramolecular structures of 1:1 iodine adducts from **1a**–**1d** and of a number of polyiodides that act as hosts towards cations with selenium–iodine bonds.

Reactions

Formation of "1:1 Adducts"

The stepwise addition of I_2 (in a titration-like manner) to solutions of phosphane selenides $t\text{Bu}_n i\text{Pr}_{3-n}\text{PSe}$ (**1a**–**1d**) dissolved in dichloromethane, trichloromethane, benzene, toluene, or mixtures thereof, leads, in all cases, to solutions for which the ^{31}P NMR spectra show only *one averaged* ^{31}P NMR signal with a pair of ^{77}Se satellites. The magnitudes of $^1J(^{77}\text{Se}, ^{31}\text{P})$ decrease with increasing amounts of I_2; in CD_2Cl_2 *averaged* ^{77}Se,^{31}P couplings are significantly smaller than in comparable C_6D_6 or toluene solutions. ^{77}Se NMR resonances of iodination products cannot be resolved as easily as those of the parent phosphane selenides. Adding less than 5% I_2 to the solution of any of the trialkylphosphane selenides **1** leads to severe broadening of the ^{77}Se NMR doublet signal, which is shifted slightly to lower field compared to that of pure **1**. With larger amounts of I_2 the ^{77}Se NMR signal becomes too broad to be resolved. This observation suggests kinetic lability of R_3PSe/I_2 systems, involving exchange reactions that are fast at the ^{1}H-, ^{13}C-, and ^{31}P NMR timescales, but *in coalescence* at the ^{77}Se NMR timescale (vide infra). Crystallization from solutions prepared from selenides **1** with one equivalent of I_2 yielded red–brown and orange–brown crystalline 1:1 adducts **2a**–**2d**. Solid **2a** contains, as mentioned in the Introduction, molecular species of type **A** (10-I-2) and ions of type **C** (10-I-2 in cations and in anions) within the same crystal.[6,7] Solid **2b**–**2d** are ionic compounds (type **C**). When only half an equivalent of iodine was used on **1b** or **1d**, crystallization still furnished the 1:1 adducts. Stripping off the solvent from the reaction mixture of **1b** with 0.5 equivalents of I_2 under reduced pressure led to a solid material that showed strong infrared absorptions assignable to $\nu(C_3PSe)$ vibration modes of free **1b** (at 587 cm^{-1}) and of the adduct **2b** (at 561 cm^{-1}).

$$t\text{Bu}_n i\text{Pr}_{3-n}\text{PSe} + \text{I}_2 \longrightarrow t\text{Bu}_n i\text{Pr}_{3-n}\text{PSeI}_2 \qquad (1)$$

n = 3: **1a**
n = 2: **1b**
n = 1: **1c**
n = 0: **1d**

2a - 2d

$$\mathbf{1a} + 1.5\ \text{I}_2 \longrightarrow t\text{Bu}_3\text{PSeI}_3 \qquad (2)$$

3a

$$\mathbf{1c} + 2\ \text{I}_2 \longrightarrow t\text{Bu}i\text{Pr}_2\text{PSeI}_4 \qquad (3)$$

4c

$$\mathbf{1b}, \mathbf{1d} + 3.5\ \text{I}_2 \longrightarrow t\text{Bu}_n i\text{Pr}_{3-n}\text{PSeI}_7 \qquad (4)$$

n = 2: **5b**
n = 0: **5d**

Reactions with Excess Iodine

Addition of 1.75 equivalents of I_2 to phosphane selenide **1a** dissolved in toluene leads to precipitation of a black residue, which can be recrystallized from toluene to provide green–black single crystals with a metallic luster; these consist of a novel compound {[(tBu$_3$PSe)$_2$I]$^+$[I$_5$]$^-$} (**3a**) containing type **D** cations.[15]

Adding an excess of molecular iodine to dichloromethane solutions of **1b**–**1d** leads to colored solutions exhibiting ^{31}P NMR singlet signals that are accompanied by satellites associated with NMR coupling constants $^1J(^{77}$Se, ^{31}P). The magnitudes of $^1J(^{77}$Se, ^{31}P) are further decreased, compared with those of the 1:1 adducts **2b**–**2d**. In a similar way, stepwise addition of iodine to suspended (partially dissolved) compounds **2b**–**2d** leads initially to deeply colored solutions, and after applying a large excess of iodine, precipitation of phosphane selenide polyiodine adducts occurs. Single crystals were isolated of green–black tBuiPr$_2$PSeI$_4$ (**4c**), dark green tBu$_2i$PrPSeI$_7$ (**5b**), and red–brown iPr$_3$PSeI$_7$ (**5d**). The bulk of product **4c** was contaminated with an unidentified dark material of higher iodine content; **5b** and **5d** were obtained analytically pure.

^{31}P- and ^{77}Se NMR Spectroscopic Investigations

Trialkylphosphane selenides (R$_3$P=Se), like their parent trialkylphosphanes (R$_3$P), exhibit ^{31}P downfield shifts that increase with increasing α-branching of the alkyl groups. Stepwise addition of iodine to **1a**–**1d** does not lead to new ^{31}P NMR signals of reaction products; rather, the singlet signal is shifted (depending on the amount of iodine) to lower frequencies (*upfield* by up to about 10 ppm, compared with **1a**–**1d**).

More indicative of the reaction course of phosphane selenides with electrophiles are coupling constants $^1J(^{77}$Se, ^{31}P), which can be determined from satellite doublets in the ^{31}P NMR spectra. In dissolved 1:1 adducts **2a**–**2d**, $^1J(^{77}$Se, ^{31}P) is about 15–20% smaller that in the parent phosphane selenides. The [R$_3$PSeI]$^+$ cations of **5b** and **5d** (in CH$_2$Cl$_2$/C$_6$D$_6$ solutions) exhibit coupling constants $^1J(^{77}$Se, ^{31}P) that are about 25% less than those of the parent selenides **1b** and **1d**; these averaged couplings are nearly as small as those of the related (10-Se-3) compounds tBu$_n i$Pr$_{3-n}$PSeBr$_2$ (see Table 1), which contain "ylidic" PSe single bonds.[11] The decrease in $^1J(^{77}$Se, ^{31}P) on coordination with increasing amounts of iodine correlates fairly well with the decrease in P–Se bond order (see the section Structure Determinations).

The observation of ^{77}Se NMR signals from compounds **2**–**5** is affected by extreme line broadening. On addition of less than 5 mol-% of I$_2$ as electrophile to **1b** in CH$_2$Cl$_2$, the ^{77}Se NMR doublet broadens and shifts slightly to lower field [δ^{77}Se = –397 ppm, J(Se, P) = 663 Hz]; with 10 mol-% I$_2$, severe broadening of the doublet (δ^{77}Se = –386 ppm) precludes the accurate determination of $J(^{77}$Se, ^{31}P). With more iodine the ^{77}Se signal becomes undetectably broad. This may be attributed to iodine exchange reactions (such as iodine transfer between phosphane selenide ligands and complexes and/or between molecular and ionic species) that are fast at the ^{1}H-, ^{13}C- and ^{31}P NMR timescales, but *in coalescence* at the ^{77}Se NMR timescale.

A ^{77}Se NMR measurement with an unusually large number of scans on pure tBu(iPr)$_2$PSeI$_2$ (**2c**), dissolved in CD$_2$Cl$_2$, allowed the resolution of the ^{77}Se NMR doublet signal at –61.3 ppm, i.e. 432 ppm downfield from that for ligand **1c** (δ^{77}Se = –493 ppm in CH$_2$Cl$_2$).[11]

Crystalline **4c** is not sufficiently soluble in dichloromethane to allow resolution of the ^{77}Se NMR doublet signal. After adding an excess of iodine to suspended **4c**, the solution exhibits a broadened ^{77}Se NMR doublet further downfield at +12 ppm. The coordination shifts $\Delta\delta$ [Δ(adduct) – Δ(ligand)] of the donating ^{77}Se nucleus in **2c** ($\Delta\delta$ = +432 ppm) and in **4c** (with an excess of I$_2$) ($\Delta\delta$ = +505 ppm) are larger than those of mesitylenetellurenyl iodide (MesTeI) adducts of **1c**[17] (see Table 2), but smaller than those of formally related trialkylphosphane selenide dibromides R$_3$PSeBr$_2$ ($\Delta\delta$ up to +1000 ppm).[11] The latter exhibit type **B** structures (see Scheme 1) with a three-coordinate selenium atom (10-Se-3).

Table 2. ^{77}Se NMR shifts δ [ppm] and coordination shifts $\Delta\delta$ [ppm] from iodine adducts and tellurenyl iodide adducts of **1c**.

	δ^{77}Se [ppm]	$\Delta\delta^{77}$Se [ppm]	$^1J(^{77}$Se, ^{31}P) [Hz]	δ^{31}P [ppm]
tBuiPr$_2$PSe (**1c**)[a]	–493		696	79.5
tBuiPr$_2$PSeI$_2$ (**2c**)[a]	–61.3	+432	566	72.8
tBuiPr$_2$PSeI$_4$ (**4c**)[a]	not sufficiently soluble in CD$_2$Cl$_2$			73.5
4c (with excess I$_2$)[a]	+12.0 (br.)	+505	539	73.6
tBuiPr$_2$PSe-MesTeI[b]	–297 (br.)	+196	626	75.3
tBuiPr$_2$PSe(MesTeI)$_2$[b]	–280 (br.)	+213	611	73.8
[tBuiPr$_2$PSeTeMes] SbF$_6$[b]	–28 (br.)	+465	500	73.8

[a] In CD$_2$Cl$_2$ or CH$_2$Cl$_2$ solvent. [b] In CDCl$_3$.

Table 1. ^{31}P NMR shifts [ppm] and coupling constants $^1J(^{77}$Se, ^{31}P) [Hz] (J values are in italics) of phosphane selenides, R$_3$PSe, **1a**–**1d**, of phosphane selenide dibromides, R$_3$PSeBr$_2$, of phosphane selenide diiodides, R$_3$PSeI$_2$, **2a**–**2d**, and of phosphane selenides with excess iodine, R$_3$PSeI$_x$ ($x > 2$), **3a**–**5d**. Solvent: CH$_2$Cl$_2$ or CD$_2$Cl$_2$.

	R$_3$PSe δ^{31}P, $\lvert^1J$(Se, P)$\rvert$	**R$_3$PSeBr$_2$** δ^{31}P, $\lvert^1J$(Se, P)$\rvert$	**R$_3$PSeI$_2$** δ^{31}P, $\lvert^1J$(Se, P)$\rvert$	**R$_3$PSeI$_x$** ($x > 2$) δ^{31}P, $\lvert^1J$(Se, P)$\rvert$
tBu$_3$PSe (**1a**)	93.3, *693*	83.0, *514*	83.6, *576.4*	82.9, *565* (**3a**)
tBu$_2i$PrPSe (**1b**)	84.4, *688*	82.9, *520*	76.8, *547*	76.1, *544* (**4b**)[a] 76.5, *528* (**5b**)
tBuiPr$_2$PSe (**1c**)	79.5, *696*	77.4, *526*	72.8, *567*	73.5, *526* (**4c**)
iPr$_3$PSe (**1d**)	70.6, *692*	69.8, *521*	65.3, *556*	66.1, *529* (**4d**)[a] 66.5, *518* (**5d**)

[a] Solution containing R$_3$PSe with two equivalents of I$_2$.

These large coordination shifts (Δδ) correspond to ^{77}Se nuclei participating in ligand exchange reactions in solution at frequency differences Δ*v* in the range 15–40 kHz, at a spectrometer frequency of 38 MHz (for ^{77}Se). Much smaller Δ*v* values in ^{1}H-, ^{13}C-, and ^{31}P NMR spectroscopy allow the resolution of sharp lines, because of averaging by fast exchange.

The *fast* ^{77}Se NMR exchange occurring during the titration-like iodination of a P=Se function had until now only been observed when the bidentate phosphane selenide $[Ph_2P(Se)]_2CH_2$ (dppmSe_2) was treated with iodine.[16] Steady ^{77}Se downfield shifts accompanied by a decrease in J(^{77}Se, ^{31}P) followed until 1.5 equivalents of I_2 per dppmSe_2 were consumed. At that stage, the averaged ^{77}Se resonance from the reaction mixture appeared +270 ppm downfield from that of "free" dppmSe_2.[16] In complexes of **1a**–**1d** with arenetellurenyl iodides (see Table 2), ^{77}Se coordination shifts (deshielding) are up to +150 ppm for 1:1 complexes and up to +300 ppm for 1:2 products such as ionic $[R_3PSeTeR]^+[RTeI_2]^-$. In these cases, broad ^{77}Se NMR doublet signals could be resolved even in reaction mixtures.[17]

Presumably, iodine exchange mechanisms at R_3PSe ligands could be related to those in trialkylphosphane-dihalogen equilibrium systems (R_3P/R_3PX_2; X = Br, I).[11,16,18] These systems involve nucleophilic attack of phosphorus ($R_3P{\rightarrow}X{-}PR_3^+$) at halogen atoms in α position with respect to the "onium" P atom center, whereas in the R_3PSe cases, the selenium attack will occur in β position ($R_3PSe{\rightarrow}X{-}SePR_3^+$) with respect to the "onium" center. Br^+ transfer transition states $[R_3PSeBrSePR_3]^+$ have recently been described on the basis of theoretical methods as "fairly accessible",[11] and cations $[R_3PSeISePR_3]^+$ can even be ground-state species in equilibria with molecular iodine complexes, as shown in the present study.[6,7,15]

Structure Determinations

1:1 Complexes

tBu₃PSeI₂ (2a)

Dark red–brown crystals of **2a** were obtained by the diffusion method (dichloromethane/*n*-hexane). The overall composition is tBu$_3$PSeI$_2$, but in fact two substructures are present: molecular tBu$_3$PSeI–I and ionic $[(t\text{Bu}_3\text{PSe})_2\text{I}]^+[\text{I}_3]^-$ (Figure 1a). The space group is $P\bar{1}$; the uncharged molecules lie on general positions, whereas the anions and cations display crystallographic inversion symmetry. The overall composition is thus $[t\text{Bu}_3\text{PSeI–I}]_2\cdot\{[(t\text{Bu}_3\text{PSe})_2\text{I}]^+[\text{I}_3]^-\}$, for which $Z = 1$. It should be noted that the reported compositions of oligo- and polymeric species are to some extent arbitrary (e.g. the composition that we have chosen for **2a** could be halved), and the Z values depend on the composition.

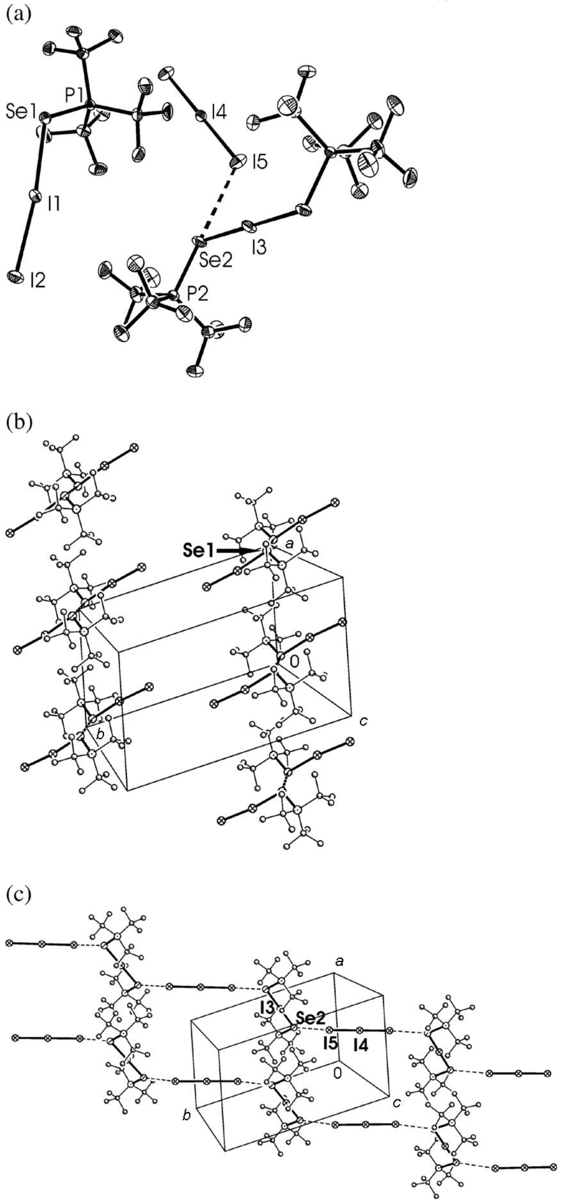

Figure 1. (a) Asymmetric unit of **2a**, selected bond lengths [Å] and angles [°]: P1–Se1 2.195(1), Se1–I1 2.760(1), I1–I2 2.915(1), Se1–I1–I2 171.69(1), P1–Se1–I1 113.33(3), Se2–I3 2.765(1), Se2–P2 2.194(1), I4–I5 2.914(1), P2–Se2–I3 109.10(3). (b) Centrosymmetric pairs of molecular complexes in solid **2a**, Se1···Se1′ 3.527(1) Å. (c) Cation–anion motif in solid **2a**, Se2···I5 4.057(1) Å. Same view direction as in (b).

The uncharged component tBu$_3$PSeI–I is related to the charge transfer adducts, numerous examples of which are known for organic sulfur and selenium ligands. In contrast to the pairs of molecules in both phases of Ph$_3$PSeI–I,[5] which exhibit long intermolecular Se···I contacts (about 3.9 Å), the tBu$_3$PSeI–I unit in **2a** is part of a centrosymmetric dimer arising from a Se1···Se1′ *van der Waals* contact of 3.527(1) Å; the dimers occupy the region $z \approx 0$ (Figure 1b). The associated angles I1–Se1···Se1′ 84.09(2)° and P1–Se1···Se1′ 138.95(3)° allow Se···Se p orbital interactions. The widened angle P1–Se1–I1 113.33(3)° reflects steric repulsion from the tBu$_3$P moiety. Charge-transfer adduct formation (n→σ* attack) usually occurs with concomitant I–I bond lengthening, the extent of which depends on the donor ability of the ligand. In $t\mathrm{Bu_3PSeI{-}I}$, the I–I bond is lengthened from 2.715 Å (solid I_2) to 2.915(1) Å, i.e. analogous to a symmetric triiodide structure, and similar to that of the I_3^- ions in **2a**, with I–I bond order 0.5.

The centrosymmetric cation $[(t\mathrm{Bu_3PSe})_2\mathrm{I}]^+$ in **2a** exhibits nearly the same Se–I distance, 2.765(1) Å, as that of the molecular adduct [2.760(1) Å], confirming that this distance is equivalent to an Se–I bond order of 0.5. The $[(t\mathrm{Bu_3PSe})_2\mathrm{I}]^+$ cations and I_3^- anions exhibit *van der Waals*-type Se···I contacts with Se2···I5 4.057(1) Å; the P2–Se2···I5 angle is approximately linear at 156.39(3)°, whereas the Se2···I5–I4 angle is much narrower at 128.52(2)°. The cation–anion adduct has a degree of freedom in the torsion angle I3–Se2···I5–I4, which is –139.54(2)°, but has appreciably different values in other related derivatives (see below). The Se2···I5 contact leads to an extended chain topology parallel to [110] in the region $z \approx {}^1/_2$ (Figure 1c). Cations with linear Se–I–Se arrangements related to that in **2a** were previously observed in ${}^1/_x[\mathrm{Se_6I^+}]_x[\mathrm{AsF_6}]^-$ [Se–I distance 2.736(3) Å; bond order ca. 0.5][19a] and in ionic compounds $[\mathrm{L_2I}]^+[\mathrm{I_3}]^-$ [L = *N*-methylbenzothiazole-2(3*H*)-selone].[19b]

tBu₂iPrPSeI₂ (2b)

Triclinic **2b** (Figure 2a) was crystallized by pentane vapor diffusion into a dichloromethane solution. The cell contains one formula unit; the I_3^- anion and the $[(t\mathrm{Bu_2}i\mathrm{PrPSe})_2\mathrm{I}]^+$ cation both display inversion symmetry. Similar to the ionic substructure of **2a**, the ions are connected by Se···I contacts [Se···I3 3.8802(5) Å] leading to chains involving ···Se–I–Se···I–I–I···Se–I–Se···I–I–I··· arrays with nearly linear I3···Se–P arrangements 175.473(8)° and bent I2–I3···SeI1 120.379(8)° (see Figure 2b). The torsion angle I1–Se···I3–I2 is 163.39(1)°. The chain direction is parallel to $[11\bar{1}]$. Compared with that in **2a**, the Se···I contacts in **2b** are 0.18 Å shorter, whereas the I–I and Se–I bonds are both marginally longer (0.02 Å). The cation bond angle I1–Se–P is 103.940(17)°, i.e. narrower than I3–Se2–P2 109.10(3)° in the cation of the bulkier **2a**.

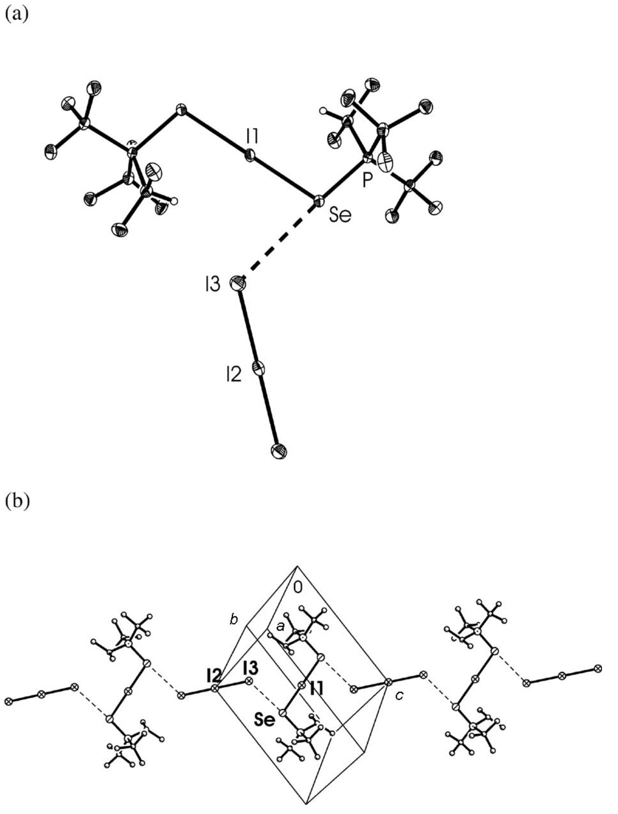

Figure 2. (a) Asymmetric unit of **2b**, selected bond lengths [Å] and angles [°]: Se–I1 2.7834(3), Se–P 2.2052(6), I2–I3 2.9336(3), P–Se–I1 103.940(17). (b) Cation–anion chain structure of **2b**, Se···I3 3.8802(5)Å. View direction perpendicular to $(1\bar{1}0)$.

The presence of C–H moieties together with iodine atoms in all these structures means that C–H···I contacts, which could be interpreted as weak hydrogen bonds, are, in principle, possible. In Figure 2a, one methine hydrogen atom at each isopropyl group is included as an indication of intramolecular H1···I1 contacts of 3.04 Å. We have previously postulated that such contacts in bromine systems may have a significant effect on the conformation.[11] In the current structure **2b**, only one H···I contact is observed between different moieties, and it is quite long with a value of 3.34 Å. For some of the other compounds, notably the tris(*tert*-butyl) derivatives, many such contacts are present (and also a small number of C–H···Se contacts). We assume these contacts to be less structure-determining than the soft–soft interactions and therefore do not discuss them in detail.

tBuiPr₂PSeI₂ (2c)

Two crystallographically independent units of $[(t\mathrm{Bu}i\mathrm{Pr_2PSe})_2\mathrm{I}]^+[\mathrm{I_3}]^-$ are present in the space group $P2_1/c$; there is no imposed crystallographic symmetry (see Figure 3a). All P–Se, Se–I, and I–I distances in **2c** are similar to those observed in **2b**, and the cation bond angles I–Se–P in **2c** are marginally smaller (by 1–2°) than those observed in bulkier **2b**. The cations display markedly different conformations, with torsion angles P1–Se1···Se2–P2 162.6(1)° and P3–Se3···Se4–P4 102.7(1)°; the analogous torsion angles in **2a** and **2b** are exactly 180° by symmetry. Within the asymmetric unit, the cation–anion contact Se1···I3 4.0138(12) is clearly identifiable and the associated angles are, as above, linear at selenium and bent at the triiodide [I3···Se1–P1 175.71(7) and I4–I3···Se1 135.65(3)°, torsion angle I1–Se1···I3–I4 96.44(4)°].

The cation–anion packing pattern in ionic $[(t\mathrm{Bu}i\mathrm{Pr_2PSe})_2\mathrm{I}]^+[\mathrm{I_3}]^-$ (**2c**) is made up from two different, and to a good approximation independent, types of chain-like arrays. One array, involving the first formula unit (top left in Figure 3a) is related to the ···Se–I–Se···I–I–I··· arrays in **2a** and **2b** (Figure 3b). In addition to the Se1···I3 contact within the asymmetric unit, atom Se2 makes a contact to I5 of the neighboring asymmetric unit related by the *c* glide plane [Se2···I5′ 3.9966(11) Å, I5′···Se2–P2 179.44(7), I4′–I5′···Se1 124.23(3)°, torsion angle I1–Se2···I5′–I4′ 91.67(3)°]. The overall effect is to form corrugated chains parallel to the *z* axis, which in turn form layers parallel to the *yz* plane at $x \approx 1/8$, 7/8. The second type of corrugated

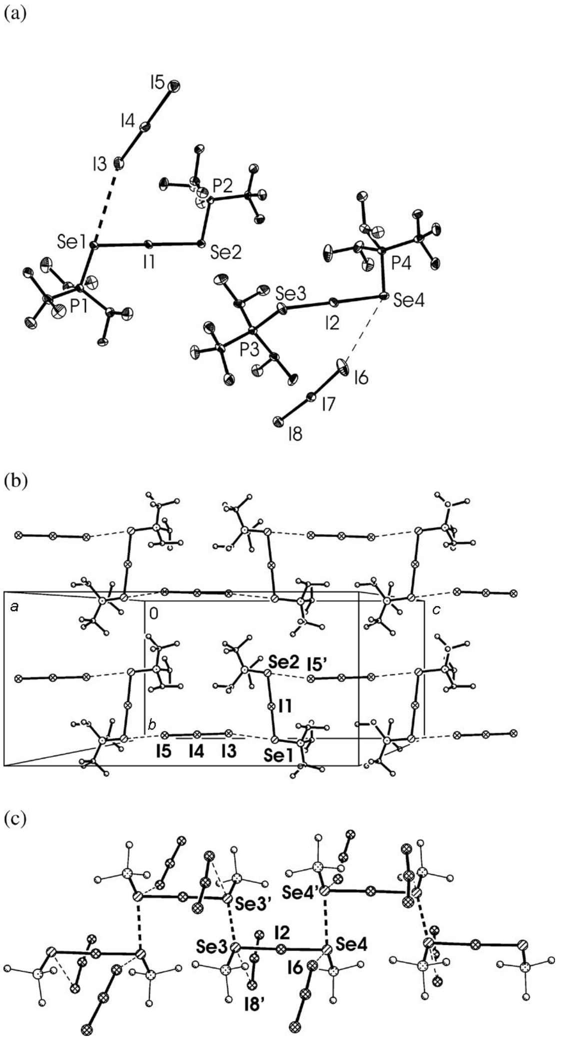

Figure 3. (a) Asymmetric unit of **2c**, selected bond lengths [Å] and angles [°]: Se1–I1 2.7733(11), Se2–I1 2.7793(10), I3–I4 2.9295(9), I4–I5 2.9122(9), Se3–I2 2.7756(11), Se4–I2 2.7910(11), I6–I7 2.9098(10), I7–I8 2.9279(9), Se1···I3 4.0138(12), Se4···I6 4.2747(13). (b) Cation–anion chain motif in solid **2c**, Se2···I5′ 3.9966(11) Å. View direction perpendicular to (100), region $x \approx 1/8$. (c) Cation–cation chain motif in solid **2c**, Se3···Se3′ 3.4355(17) Å, Se4···Se4′ 3.5856(18) Å. View direction approximately parallel to the *z* axis. The phosphane substituents are reduced to the *ipso* carbons for clarity.

chain, parallel to the *y* axis at $x \approx ½$, involves the cations of the second formula unit (bottom right in Figure 3a), which are connected by secondary Se···Se contacts across inversion centers [Se3···Se3′ 3.4355(17) Å, Se4···Se4′ 3.5856(18) Å; see Figure 3c]. These Se···Se soft–soft interactions are comparable to those observed in the "dimers" [tBu$_3$PSeI–I]$_2$ in molecular **2a** and in the chains of $^1/_x$[Se$_6$I$^+$]$_x$-[AsF$_6$]$^-$ [Se···Se 3.591(3) Å].[19a]

It is a well-known problem in the analysis of crystal packing motifs involving secondary contacts that van der Waals radii can neither be exactly determined nor rigidly applied, so there is no exact criterion for defining a significant contact. The packing analysis may in some cases be carried out conservatively in terms of only the shortest and most-striking contacts; the alternative extreme, of considering even contacts appreciably longer than the sum of the van der Waals radii, has the potential disadvantage that important features may disappear under a welter of detail. For compound **2c**, standard search criteria revealed the contacts shown in Figure 3b, even though they are approximately 4 Å long. At first sight, the cation chains shown in Figure 3c did not involve any anions. However, extending the search to longer distances revealed the very long contacts Se4···I6 4.2747(13) and Se3···I8′ 4.3197(12) Å; the former are shown in Figure 3a and both in Figure 3c. They serve to link adjacent cation chains. With increasing I···Se distance, the requirement for linearity at Se is relaxed, as would be expected; I6···Se4–P4 is 130.31(6)° and I8′···Se3–P3 108.85(6)°. It is increasingly the case that very long contacts, even if appreciably longer than secondary contacts based on the sum of the van der Waals radii, are being regarded as structurally significant (further examples will be presented below). For such systems we propose the term *tertiary contacts*.

*i*Pr$_3$PSeI$_2$ (2d)

Triclinic **2d** (see Figure 4a) is closely analogous to **2b**; it consists of inversion-symmetric (iPr$_3$PSe)$_2$I$^+$ cations and I$_3^-$ anions, which are connected by Se···I contacts [3.8644(7) Å] leading to ···Se–I–Se···I–I–I··· arrays that have nearly linear I3···Se–P [173.27(3)°] and bent I2–I3···Se moieties [114.579(15)°, see Figure 4b]. The chains thus formed are

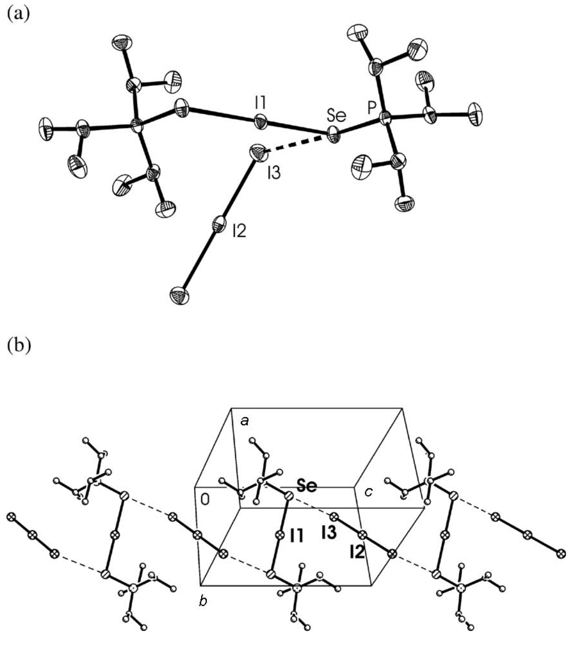

Figure 4. (a) Asymmetric unit of **2d**, selected bond lengths [Å] and angles [°]: Se–I1 2.7771(5), Se–P 2.1905(10), I2–I3 2.9083(4), P–Se–I1 103.52(3). (b) Cation–anion chain structure of **2d**, Se···I3 3.8644(7) Å. View direction perpendicular to (110) in the region $x,y \approx ¼$.

parallel to the *z* axis. The structures **2b** and **2d** are, however, *not* isotypic, as can be seen, e.g. from the I1–Se···I3–I2 torsion angle of –73.564(15)° in **2d**, compared to the corresponding torsion angle of 163.39(1)° in **2b**. The P–Se and Se–I bond lengths and the P–Se–I angle are similar to those in **2b**. The close analogy between **2b** and **2d** is remarkable in view of the fact that the sterically "intermediate" derivative **2c** exhibits a different cation–anion packing pattern including Se···Se contacts. Exchange of *tert*-butyl for isopropyl groups at the phosphorus atom also has a large impact on the supramolecular structures of iodophosphonium salts $[t\mathrm{Bu}_{2-n}i\mathrm{Pr}_n\mathrm{PI}_2]\mathrm{I}$ (n = 0, 1, 2)[18] and phosphane selenide dibromides $t\mathrm{Bu}_n i\mathrm{Pr}_{3-n}\mathrm{PSeBr}_2$.[11]

The observation that our trialkylphosphane selenide 1:1 complexes with I_2 are preferably ionic adducts that exhibit Se–I and I–I bond orders of about 0.5 (symmetric 3c–4e systems, as is *molecular* **2a**), whereas tris(dialkylamino)phosphane selenides (stronger donors) as well as triarylphosphane selenides and $t\mathrm{Bu}_2\mathrm{P(Se)I}$ (weaker donors) lead to molecular adducts[5–7] with "unsymmetric" 3c–4e systems represents a challenge to further theoretical and experimental work.

Compounds Arising from More Than One Equivalent of Diiodine

$t\mathrm{Bu}_3\mathrm{PSeI}_3$ (3a)

Single crystals of composition $(t\mathrm{Bu}_3\mathrm{PSe})_2(\mathrm{I}_2)_3(\mathrm{CH}_3\mathrm{C}_6\mathrm{H}_5)$ were isolated from a toluene solution of compound **2a** with excess iodine as green prisms with a metallic sheen. They proved to contain the ionic compound $[(t\mathrm{Bu}_3\mathrm{PSe})_2\mathrm{I}]^+[\mathrm{I}_5]^-$ (**3a**) as a toluene hemisolvate (see Figure 5a) crystallizing in the space group *C*2/*c* with one formula unit in the asymmetric unit.[15] In contrast to the inversion-symmetric $(t\mathrm{Bu}_3\mathrm{PSe})_2\mathrm{I}^+$ ions in the ionic substructure of **2a**, the cations in **3a** are not strictly linear [Se1–I1–Se2 170.27(3)°], and the phosphonium centers in **3a** are oriented in a *cisoid* fashion (torsion angle P1–Se1···Se2–P2: 67.4°). This conformation allows the cations to undergo pairing across a twofold axis through weak Se1···Se2′ interactions [3.6795(14) Å, see Figure 5b]. These are related to the Se···Se contacts in pairs of *molecular* **2a** and in one substructure of ionic **2c**, where arrays of cations are built through Se···Se contacts. Formally related cations with approximately linear coordination of the central atom are

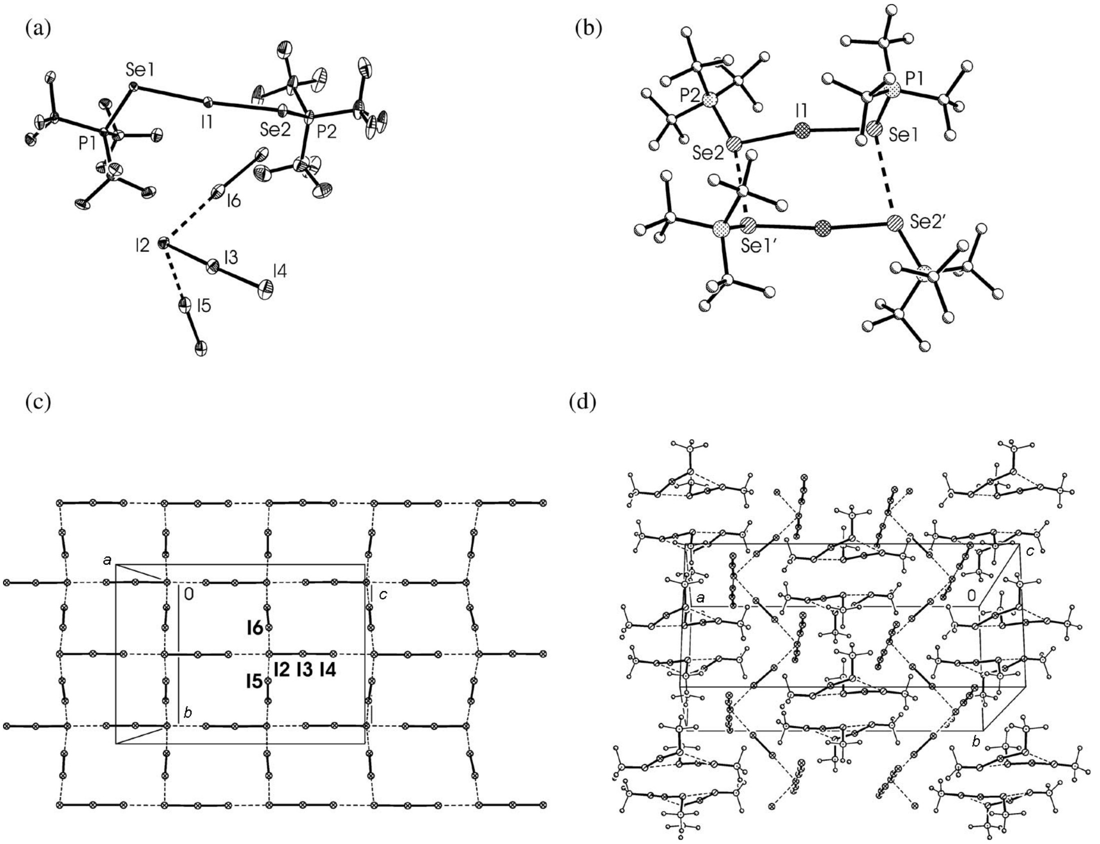

Figure 5. (a) Cation–anion motif in solid **3a**, selected bond lengths [Å] and angles [°]: Se1–I1 2.7674(11), Se2–I1 2.7374(11), I2–I3 3.0977(12), I3–I4 2.8196(13), I5–I5′ 2.7746(19), I6–I6′ 2.7760(19), Se1–I1–Se2 170.27(3), I2···I5 3.4105(12), I2···I6 3.4276(12). The disordered toluene molecule is omitted. The asymmetric unit is extended to complete the diiodine molecules at I5 and I6. Ellipsoids correspond to 30% probability levels. (b) Centrosymmetric pair of cations in **3a**: Se1···Se2′ 3.6795(14) Å. (c) Topology of a corrugated I_5^- sheet in **3a**: I2···I4′ 3.7791(13) Å. View direction perpendicular to (100). (d) Packing diagram of **3a**. View direction approximately perpendicular to (001).

known from the coordination chemistry of gold(I) and silver(I) with chalcogen ligands.[20,21] The cation in [(Ph$_3$-PSe)$_2$Au]SbF$_6$ is strictly monomeric,[20] whereas two-coordinate silver(I) phosphane selenide cations display heteronuclear Ag···Se cation–cation contacts;[21] the pairwise attraction through (homonuclear) Se···Se (ligand–ligand) contacts in **3a** is unique. The pairs of (tBu$_3$PSe)$_2$I$^+$ cations are packed in channels between the corrugated layers of a novel type of pentaiodide structure. The corrugated I$_5^-$ layers can be regarded as approximately linear parallel chains of very asymmetric I$_3^-$ anions [···I4–I3···I2···]$_x$ {I2–I3 3.0977(12) Å, I3–I4 2.8196(13) Å} that are connected through bridging iodine molecules [I5–I5′ 2.7746(19) Å, I6–I6′ 2.7760(19) Å], both of which lie across inversion centers. The “iodide” ion I2 exhibits a sawhorse-like coordination mode with contacts towards four iodine molecules: a stronger (see above) and a very weak contact, I2···I4′ 3.7791(13) Å, within the “triiodide chain”, and two contacts, I2···I5 3.4105(12) Å, I2···I6 3.4276(12) Å, to the bridging diiodine molecules (see Figure 5c). The sawhorse-like coordination mode of I2 enables the polymeric I$_5^-$ structure to generate corrugated layers in the regions $x \approx$ ¼, ¾. Face-to-face packing of the layers is apparently a template effect from the pairs of [(tBu$_3$PSe)$_2$I]$^+$ cations, which, together with disordered toluene, find optimal space in the channels thus created (see Figure 5d).

*t*Bu*i*Pr$_2$PSeI$_4$ (4c)

Adding one equivalent of iodine to **1c** leads to crystallization of **2c** from CH$_2$Cl$_2$ solutions; on adding a large excess of iodine, a brown–red solid separates from the colored solution. The C, H analytic composition of the bulk precipitate corresponds to a formulation somewhere between the adducts tBuiPr$_2$PSeI$_4$ and tBuiPr$_2$PSeI$_5$; the precipitate contained a few crystals that were suitable for X-ray diffraction. The crystalline compound tBuiPr$_2$PSeI$_4$ (**4c**), space group $P2_1/c$, is a 1:2 adduct of **1c** with iodine molecules. Two crystallographically independent 1:1 adducts tBuiPr$_2$-PSeI–I are connected by two additional diiodine molecules (see Figure 6a).

The tBuiPr$_2$PSeI–I units are distorted, compared with molecular **2a**. They represent very unsymmetric 3c–4e systems (Se–I 2.62–2.63 Å; I–I 3.13–3.15 Å). Alternatively, they may be regarded as pairs of strongly interacting ions tBuiPr$_2$PSeI$^+$···I$^-$, whereby the iodide ion exhibits a secondary $n_I \rightarrow \sigma_{Se-I}^*$ interaction with the tBuiPr$_2$PSeI$^+$ cation (Se–I bond order >>0.5, I–I bond order <<0.5) and is also in contact with two I$_2$ molecules. In the formula unit containing Se1 (tBuiPr$_2$P1Se1–I1–I2), one additional contact with Se2 is formed [I2···Se2′ 4.0693(5) Å]. Accordingly, the formal “iodide” I2 is μ$_4$-bridging between the iodine atom of the cation [I1···I2 3.1292(4) Å], the Se2′ atom (see above), and two I$_2$ molecules [I2···I8′ 3.4798(3) Å; I2···I5 3.3440(3) Å], see Figure 6e). The atom I4, the iodide of the second formula unit, is μ$_3$-bridging (trigonal pyramidally) between the iodine atom of its cation [I3···I4 3.1423(4) Å] and two I$_2$ molecules [I4···I6 3.5302(3) Å; I4···I7 3.2460(3) Å], if we ignore the longer tertiary contact I4···Se1′ 4.1950(5) Å (see Figure 6d). The structure of **4c** differs from that of the other known 1:2 adduct (Me$_2$N)$_3$PSeI$_4$, which consists of [(Me$_2$N)$_3$P$^+$–Se–I···I$^-$···I–I] moieties.[4] The latter contain stronger Se–I bonds than **4c**, and they exhibit only very weak additional I···I and Se···I contacts (> 3.7 Å). The μ$_3$-bridging role of I$^-$ in **4c** between iodine atoms from one cation and two I$_2$ molecules is related to that in (Morph)$_2$PSeI$_5$.[4] The local environment of I$^-$ in this system is also structurally reminiscent of some I$_7^-$ ions that feature a central I$^-$ interacting with three iodine molecules with an approximate local C_{3v} symmetry.[19b,22]

For an analysis of the packing, it is advantageous to consider two formula units separately. One of the tBuiPr$_2$PSe units (based on Se1) leads with one I$_2$ molecule (I5–I6) to “dimeric” moieties [···Se(PtBuiPr$_2$)–I–I···I–I···]$_2$. The inversion-symmetric *pairs* are connected through Se1···I6′ [3.6427(5) Å] and I2···I5 [3.3440(3) Å] contacts (Figure 6b). They lie in layers parallel to the xy plane at $z \approx 0,½,1$, etc. The other half of the tBuiPr$_2$PSe units (based on Se2), together with the other iodine molecule (I7–I8), associate via the 2$_1$ axis to form a chain parallel to the y axis, with Se2···I8′ [3.7707(4) Å] and I4···I7 [3.2460(3) Å] (Figure 6c). The chains lie in the regions $z \approx$ ¼, ¾. The interface between the two packing motifs involves the interaction I2···I8′ [3.4798(3) Å] and the long contacts Se2′···I5 and Se2′···I2 [4.0600(4) and 4.0693(5) Å], leading to zigzag chains of molecules parallel to the y axis (Figure 4d and e) in the regions $z \approx 1/8$, etc. The tertiary contact Se1···I4 [4.1950(5) Å] can be seen implicitly in Figure 4d; it links neighboring chains.

The structure of **4c** represents the case of a *transition* from molecular complexes, such as Ph$_3$PSe–I–I and (R$_2$N)$_3$-PSe–I–I,[5] to compounds [(R$_2$N)$_3$PSe–I]$^+$···I$_x^-$ (x = 3, 4)[4] and [tBu$_n$$iPr_{3-n}$PSe–I]$^+$···I$_x^-$ (x = 6, n = 2 and 0: **5b**, **5d**, vide infra) that exhibit increased cation–anion separation.[15]

*t*Bu$_2$*i*PrPSeI$_7$ (5b)

Compound **5b** crystallizes in the orthorhombic space group $P2_12_12_1$ and thus can have no imposed symmetry. The asymmetric unit may be summarized as containing two tBu$_2$$i$PrPSeI$^+$ cations (iodine atoms I1 and I2), two iodides (I3 and I4), and five diiodine molecules (I5–14) It was chosen in such a way as to maximize the coordination number at the iodides (within the asymmetric unit).

The cation–anion separation is better expressed in **5b** than in any of the phosphane selenide iodine adducts with lower iodine content. Cationic tBu$_2$$i$PrPSeI$^+$ moieties, related to the (tuI)$_2$I$^+$ cations in (tu)$_2$I$_{10}$ (tu = thiourea),[23] consist of an iodide ion (I3) bridging two tBu$_2$$i$PrPSeI$^+$ cations [I3–I1 3.3019(5) Å and I3–I2 3.2482(5) Å]. The weakness of these interactions is explained by three further contacts of the iodide ion (I3) with iodine atoms from diiodine molecules [I3–I5 3.4848(5) Å, I3–I7 3.3695(5) Å, and I3–I8′ 3.3977(5) Å] (see Figure 7a and b). In view of the complexity of the structure, we present in Table 3 a summary of the iodine topology. However, most of the contacts cooperate to produce a formally two-dimensional, albeit far from

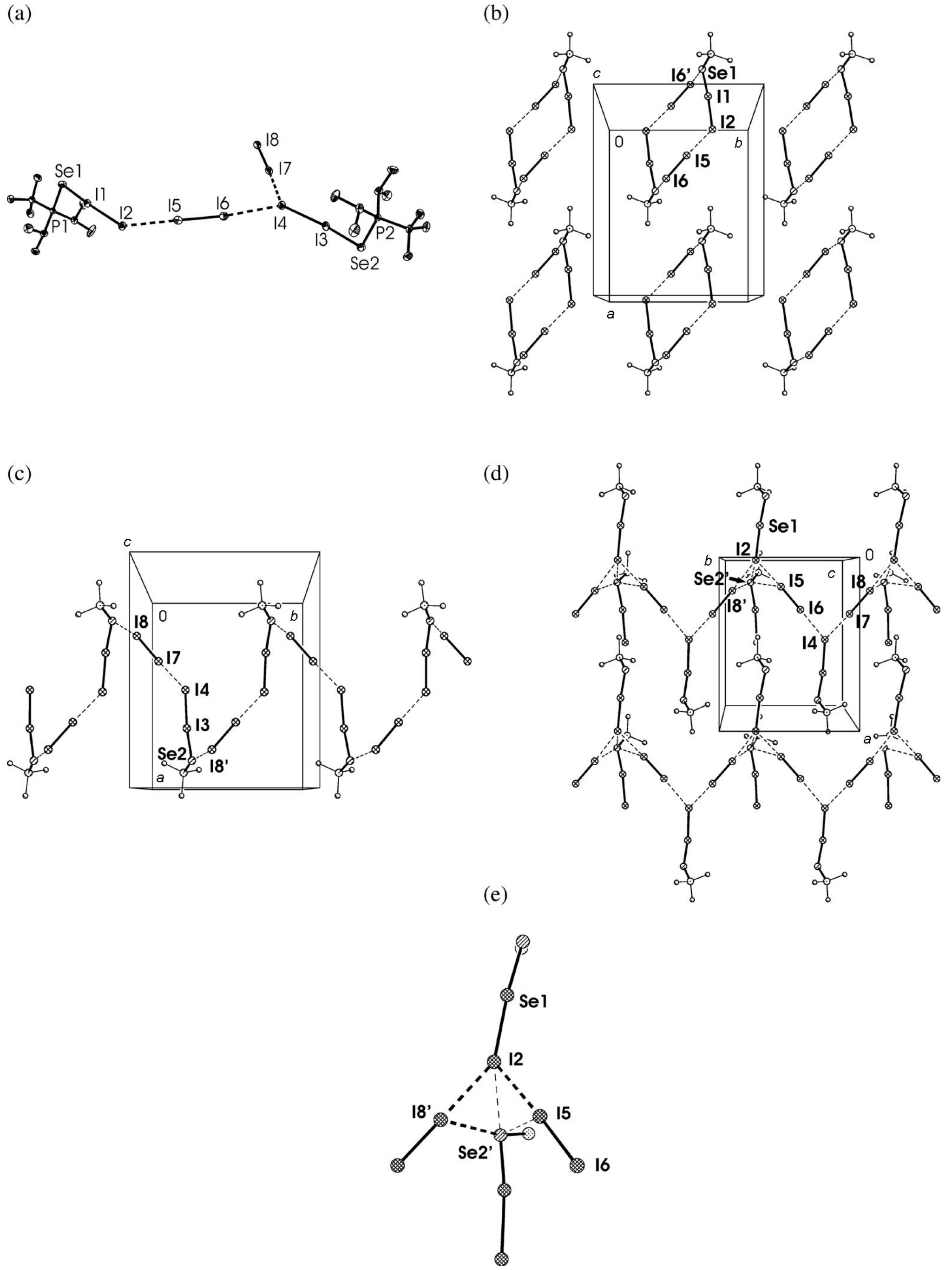

Figure 6. (a) Asymmetric unit of **4c**, selected bond lengths [Å]: Se1–I1 2.6329(4), Se1–P1 2.2117(7), Se2–I3 2.6203(4), Se2–P2 2.2119(7), I1···I2 3.1292(4), I3···I4 3.1423(4), I5–I6 2.7531(3), I7–I8 2.7694(3), I2···I5 3.3440(3), I4···I6 3.5302(3), I4···I7 3.2460(3). (b) Se1···I6′ [3.6427(5) Å] and I2···I5 [3.3440(3) Å] contacts in inversion-symmetric *pairs* in **4c** (region $z \approx 0$). View direction perpendicular to (001). The phosphane substituents are reduced to the *ipso* carbons for clarity. (c) Chain connections through Se2···I8′ [3.7707(4) Å] and I4···I7 [3.2460(3) Å] contacts in **4c**. Same view direction as in (b). The phosphane substituents are reduced to the *ipso* carbons for clarity. (d) Contacts between the regions shown in (b) and (c). Same view direction as in (b). (e) Detail of (d): connections of Se2 atoms in **4c**; Se2′···I2 [4.0693(5) Å], Se2′···I5 [4.0600(4) Å], and Se2′···I8′ [3.7707(4) Å].

planar, structure parallel to *xz* (Figure 7b). The diiodine molecule I11–I12 is directed perpendicularly to the layer and forms a contact I12···I5 to the neighboring layer (Figure 7c). There are also two SeI contacts to the neighboring layer; I9 forms a linear arrangement P2–Se2···I9 [angle 176.02(4)°, Se2···I9 3.7894(6) Å], as does I6 [P1–Se1···I6 166.55(4)°, Se1···I6 3.6449(6) Å] (see Figure 7c). Such additional P–Se···I contacts are, as seen above, a common feature of many iodine adducts of phosphane selenide.[4,6,7] I_2 molecules are also parts of linear I^-···I–I···I^- and of L-shaped $(I_2)_2$ motifs that contribute to the anion network of **5b** (see Figure 7b).

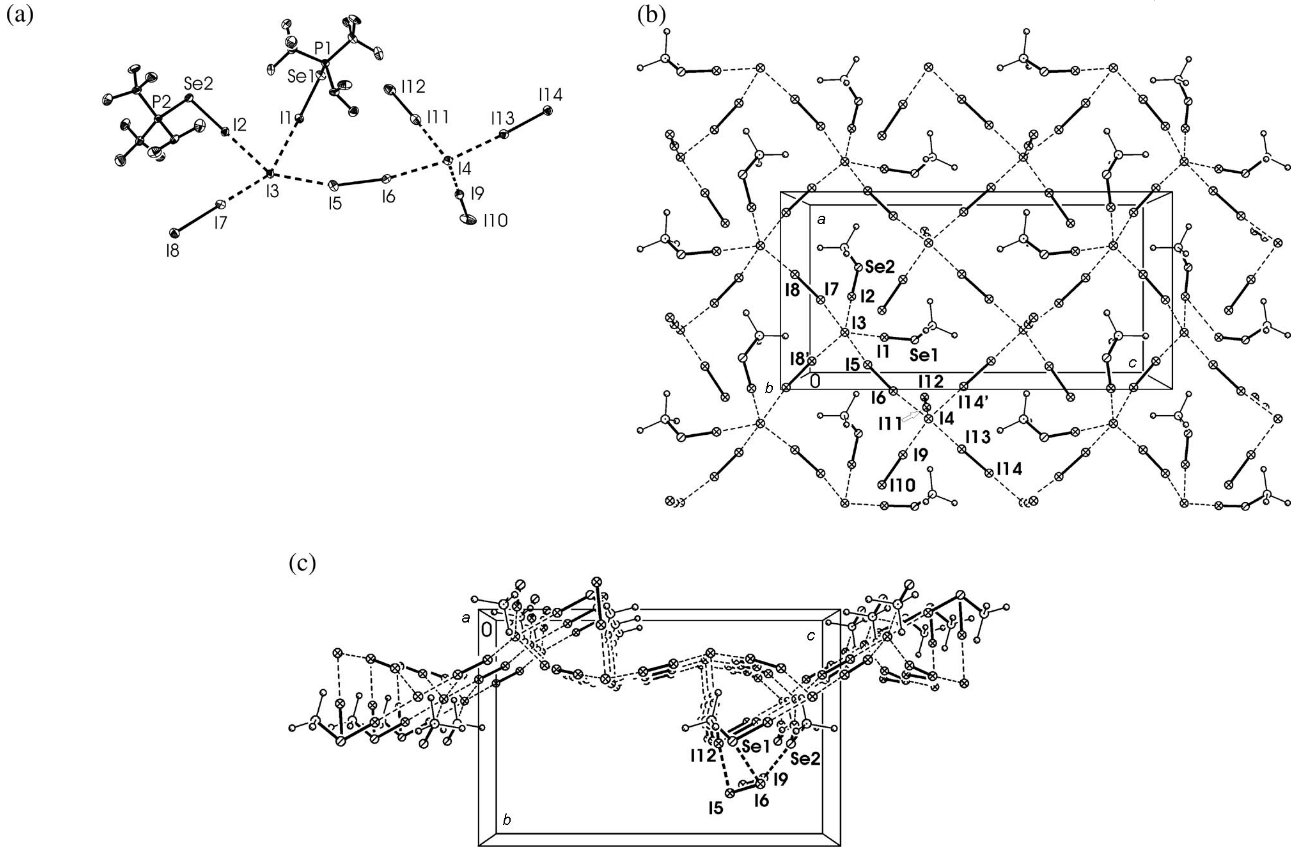

Figure 7. (a) Structure of **5b**, asymmetric unit. Selected bond lengths [Å] and angles [°]: Se1–I1 2.5635(6), Se2–I2 2.5666(6), Se1–P1 2.2349(12), Se2–P2 2.2370(12), P1–Se1–I1 102.10(3), P2–Se2–I2 101.62(4), I1···I3 3.3019(5), I2···I3 3.2482(5), I3···I7 3.3695(5), I3···I5 3.4848(5), I4···I6 3.2821(5), I4···I9 3.2579(5), I4···I11 3.4678(5), I4···I13 3.3153(5). (b) Packing through soft–soft contacts in **5b**. View direction parallel to the *y* axis. The phosphane substituents are reduced to the *ipso* carbons for clarity. (c) Interlayer connections through Se···I contacts [Se1···I6′ 3.6449(6) Å, Se2···I9 3.7894(6) Å] and I···I [I5···I12′ 3.5331(6) Å] in **5b**. View direction parallel to the *x* axis. The phosphane substituents are reduced to the *ipso* carbons for clarity.

Table 3. The topology of I–I contacts in the complex structure of **5b**.

I1, I2	CN 2; part of $t\mathrm{Bu}_2i\mathrm{PrPSeI}^+$ cations; contact to I3
I3	iodide, CN 5; linking the $t\mathrm{Bu}_2i\mathrm{PrPSeI}^+$ cations; contact to I5–I6; crosslinked to I3′ from neighboring formula units by I7–I8 and I7′–I8′, and to I4 by I5–I6
I4	iodide, CN 5; surrounded by four I_2 molecules (I5–I6, I9–10, I11–I12, I13–I14); crosslinked to I4′ by I13–I14 and I13′–I14′; crosslinked to I5 of adjacent layer by I11–I12
I5–I6	molecule, bridging I3 [from the $(t\mathrm{Bu}_2i\mathrm{PrPSeI})_2\mathrm{I}^+$ group] and I4; I5 is in contact with I12′ from an adjacent layer; the molecule is also in contact with the adjacent layer through I6···Se1
I7–I8	molecule; linking I3 with two neighboring I3′
I9–I10	molecule; I10 is terminal; I9 is linked to the adjacent layer through I9···Se2
I11–I12	molecule; I12 is in contact with I5′ of an adjacent layer
I13–I14	molecule; crosslinking I4 with two adjacent I4′

*i*Pr$_3$PSeI$_7$ (5d)

The structure of **5d** is even more complex than **5b**. It crystallizes in the orthorhombic space group *Pna*2$_1$, in which there can be no imposed symmetry. The asymmetric unit may be summarized as containing four $(i\mathrm{Pr}_3\mathrm{PSeI})_2\mathrm{I}^+$ cations (iodine atoms I1–4), four iodides (I5–8) and ten diiodine molecules (I9–28); it was chosen as above.

The character of P–Se and of Se–I bonds in the cations of **5b** and **5d** is very similar (Se–I 2.563–2.578 Å). The steric differences between the alkyl groups of the cations of **5b** and **5d** (two methyl groups fewer) lead, however, to different long-range orders of their polyiodide anion structures. Again, we present a summary of the iodine topology (Table 4). The majority of contacts (exceptions are discussed below) in the polyiodide structure of **5d** again lead to a two-dimensional structure, a puckered net consisting of condensed "squares" $[(\mathrm{I}^-)_4(\mathrm{I}_2)_4]$ (see Figure 8b). A related polyiodide network exhibiting pentacoordinate iodide anions is known.[24]

The four I^- anions (I5, I6, I7, I8 in Figure 8a) exhibit interactions with additional I_2 molecules and/or with iodine atoms of $[i\mathrm{Pr}_3\mathrm{PSeI}]^+$ cations. Iodide anion I5 is surrounded by two such cations (*i*Pr$_3$P1–Se1–I1 and *i*Pr$_3$P2–Se2–I2) and four I_2 molecules [one of the I···I$_2$ distances (I5···I9) is quite long at 3.6860(16) Å], two five-coordinate I^- anions are in contact with one cation (I6 with *i*Pr$_3$P3–Se3–I3, and I7 with *i*Pr$_3$P4–Se4–I4) and with four I_2 molecules, and the fourth I^- anion (I8) is surrounded by five I_2

Table 4. The topology of I–I contacts in the complex structure of **5d**.

I1, **I2**, **I3**, **I4**	CN 2; part of $i\text{Pr}_3\text{PSeI}^+$ cations; I···I contacts to I5, I5, I6, I7 and Se···I contacts to I14, I23, I25, I19
I5	iodide, CN 6; links the $i\text{Pr}_3\text{PSeI}^+$ cations at I1 and I2; contacts to diiodines through I9, I15, I17, I18
I6	iodide, CN 5; contact to the $i\text{Pr}_3\text{PSeI}^+$ cation at I3; contacts to diiodines through I10, I11, I16, I19
I7	iodide, CN 5+1; contact to the $i\text{Pr}_3\text{PSeI}^+$ cation at I4; contacts to diiodines through I12, I13, I20, I21; longer three-center contact to I26
I8	iodide, CN 5; contacts to diiodines through I14, I23, I24, I25, I27
I9–**I10**	molecule, bridges the iodides I5 and I6
I11–**I12**	molecule, bridges the iodides I6 and I7
I13–**I14**	molecule, bridges the iodides I7 and I8; additional contacts: I13 in three-center system I7/13/26; I14···Se1
I15–**I16**	molecule, bridges the iodides I5 and I6
I17–**I18**	molecule, bridges the iodide I5
I19–**I20**	molecule, bridges the iodides I6 and I7; additional contact: I19···Se4
I21–**I22**	molecule, terminal through I7···I21–I22
I23–**I24**	molecule, bridges the iodide I8; additional contact: I23···Se2
I25–**I26**	molecule, bridges the iodides I7 and I8; additional contacts: I26 in three-center system I7/13/26; I25···Se3
I27–**I28**	molecule, terminal through I8···I27–I28

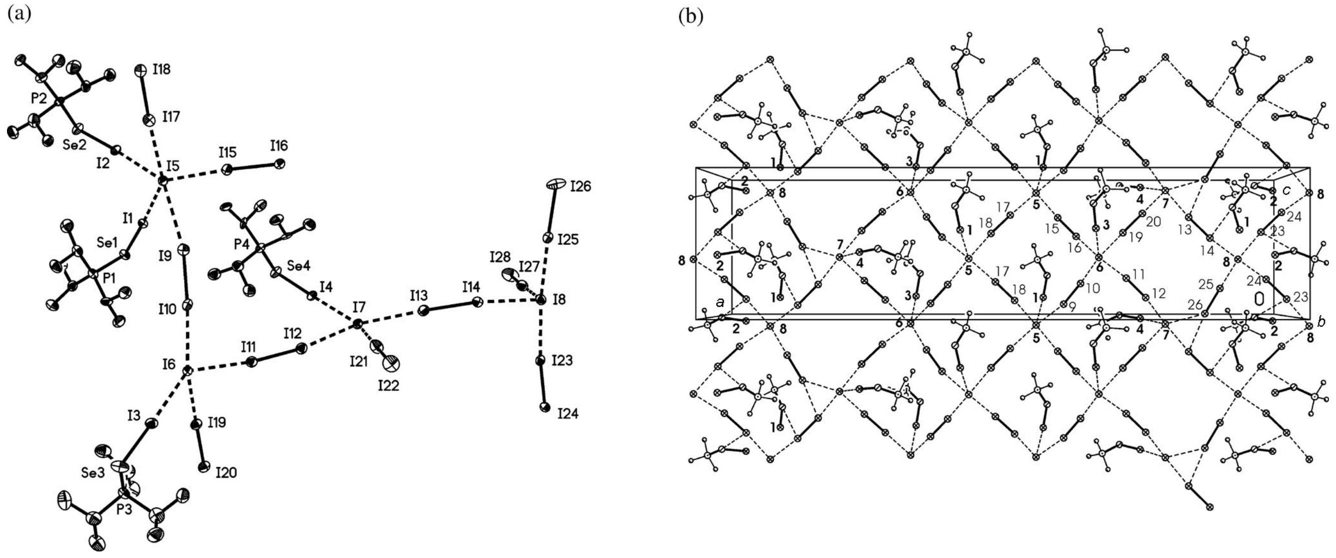

Figure 8. (a) Formula unit of **5d**, selected bond lengths [Å] and angles [°]: Se1–I1 2.5628(19), Se2–I2 2.5637(19), Se3–I3 2.571(2), Se4–I4 2.578(2), P1–Se1–I1 99.92(12), P2–Se2–I2 99.90(12), P3–Se3–I3 100.31(13), P4–Se4–I4 99.15(12), I1···I5 3.2663(15), I2···I5 3.2861(14), I9···I5 3.6860(16), I15···I5 3.4407(15), I17···I5 3.5015(16), I6···I3 3.3088(16), I10···I6 3.2641(16), I11···I6 3.4121(16), I19···I6 3.5114(15), I4···I7 3.2853(15), I12···I7 3.3488(16), I13···I7 3.3888(16), I21···I7 3.5843(15), I14···I8 3.2633(16), I23···I8 3.3763(16), I25···I8 3.1772(16), I27···I8 3.3147(16). (b) Packing diagram of **5d**. View direction perpendicular to (010). The phosphane substituents are reduced to the *ipso* carbons for clarity. Boldface numbers refer to iodines of the cations and anions, other numbers to the diiodines. The diiodines I21–I22 and I27–I28, which are directed perpendicularly away from the network, are omitted for clarity. Both types of contact (I···I and Se···I) are shown for cation **1**, but (for clarity) only Se···I for cation **2** and only I···I for cations **3** and **4**. Thus only one of the two cations at the iodide I5 (cf. Figure 8a) is shown.

molecules. At I7, the cation and one of the I_2 molecules [short I21–I22 2.6899(17) Å] are out-of-plane-oriented, leaving a "defect" in the square net. Similarly, at I8 the diiodine molecule I27–I28 is directed perpendicularly away from the net, although the bond is not as short as I21–I22; the number of tertiary contacts (I22: two of ca. 4.1–4.2 Å; I28: five from 4.1–4.4 Å) may play a role here. The only other iodine atom that is apparently terminal is I26, but this is involved in three-center interactions I7···I26 (not considered above) and I13···I26, which are rather longer at 3.821(2) and 3.850(2) Å, respectively; corresponding triangular groupings may be recognized in Figure 8. The alkyl groups function as spacers between the layers, the only interlayer soft–soft contacts are of the type P–Se···I–I (Se1···I14′, Se2···I23′, Se3···I25′, Se4···I19′), all lying in the range 3.7–4.0 Å and approximately linear at Se. There are further Se···I contacts of ca. 4.1 Å, not noted here in detail, which may be regarded as tertiary (see Figure 8b); the first two of these are included in Figure 8b. In view of the highly puckered nature of the networks and the two types of contacts (Se···I and I···I) observed for the cations, it is to some extent arbitrary which type of contact is regarded as being within the layer and which as bridging adjacent layers.

In summary, rather long cation–anion I···I distances in **5b** and **5d** (between 3.248 Å and 3.308 Å) correlate well with the shortest yet observed (P)–Se–I-bonds (2.563–2.578 Å) in the $[R_2R'P\text{–}Se\text{–}I]^+$ cations.

Vibrational Spectra

FT-Raman spectroscopy is of great help in investigating the nature of the products obtainable by reacting dihalogens/interhalogens (particularly I_2) with donor molecules containing elements of groups 15 and 16.[25–29] Indeed, the Raman peaks related to the vibration modes of the halogen-containing frameworks are generally much more intense than those of the remaining organic moieties. However, in the absence of X-ray structural data, it is necessary to be cautious in hypothesizing about the nature of the solid products on the basis of only the observed Raman peaks, since different groups may display indistinguishable vibrational patterns in the low-frequency region. This is the case, for example, for the linear three-body systems Se–I–I (in CT adducts, type **A** in Scheme 1) and I–Se–I (in hypervalent selenium adducts, type **B** in Scheme 1).[25–29] The situation is further complicated by the fact that a vibrational analogy has also been found between the above-mentioned three-body systems and the linear Se–Te–I group in complexes of bidentate phosphane selenide ligands with mesitylenetellurenyl iodide[16] and also with symmetric or slightly asymmetric I_3^-, which represents one of the most important species obtainable from the reaction of chalcogen donor molecules with I_2. The vibrational analogy observed for such different linear three-body systems containing iodine has also been established between the linear groups Br–E–Br (E = S, Se) and symmetric or slightly asymmetric trihalides XBr_2^- (X = I, Br).[25–29] This stimulates the use of the FT-Raman technique for analyzing as many crystallographically characterized compounds as possible, for each structural motif available, in order to reach a confident correlation between structural features and vibrational properties.

Among the compounds reported here, **2a**–**2d** are all characterized by the presence of symmetric or slightly asymmetric $[(t\mathrm{Bu}_n i\mathrm{Pr}_{3-n}\mathrm{PSe})_2\mathrm{I}]^+$ (n = 3: **2a**; n = 2: **2b**; n = 1: **2c**; n = 0: **2d**), bis(chalcogen)-coordinated halogen(I) complexes featuring the Se–I–Se three-body system (type **C** in Scheme 1). Unfortunately, very few spectroscopic data are available for these type **C** complexes in the literature, and generally the FT-Raman spectra are dominated by the absorption peaks of the polyiodide counteranions. Therefore, a structural/vibrational relationship has not been established.

The only isolated and characterized products from the direct reactions between chalcogen donors and dihalogens have been cations of the type $[E–X–E]^+$, which feature as a central atom only I^+ interacting with either S or Se donors.[16,30] Similarly, observations for the linear three-body system in CT adducts (E–I–Y, E = S, Se; Y = I, Br, Cl), trihalides (X–I–X, X = I, Br, Cl), and hypervalent compounds (X–E–X, E = S, X = Br, Cl; E = Se, X = I, Br, Cl), indicate that in these cations there is also an inverse correlation between the two E–I bond lengths (E = S, Se): a strengthening of one I–E bond is accompanied by a lengthening of the other, the total length of the E–I–E framework being almost independent of the nature of the substrate incorporating the chalcogen (this is consistent with a 3c–4e bonding scheme for these systems).[16,30] The mean value of the E···E distance is 5.28 Å for the S–I–S system and 5.50 Å for the Se–I–Se system [these distances are very similar to the average respective value for the sums of S–I and I–Cl in ICl adducts with S donors (5.22 Å) and Se–I and I–Br in IBr adducts with Se donors (5.53 Å)].[16,22,30] On these grounds, and considering S/Cl and Se/Br mass similarities, the Raman peaks for the stretching vibrations of the E–I–E (E = S, Se) three-body systems should occur at frequencies very close to those observed for ICl adducts with S donors or ICl_2^- trihalides (E = S), or IBr adducts with Se donors or Br_3^- and IBr_2^- trihalides (E = Se). The FT-Raman spectra of **2a**–**2d** are all dominated by the very intense absorption peak at about 113 cm^{-1} (see Experimental Section), arising from the symmetric stretching of the symmetric I_3^- counterion. In the case of **2a**, the second fairly intense peak at 123 cm^{-1} can be assigned to the symmetric stretching vibration mode of the Se–I–I three-body system in the type **A** unit.[16,22,29] The considerable intensity of these two peaks for **2a** prevents the identification of any peak at about 145 cm^{-1}, a position expected for the antisymmetric stretching vibration mode of the Se–I–I system.[16,22,29] The symmetric or slightly asymmetric Se–I–Se group, common to **2a**–**2d**, should give rise to a peak at about 160 cm^{-1}, as found for symmetric or slightly asymmetric Br_3^- and IBr_2^- trihalides (see discussion above). Indeed, all four compounds show, in their FT-Raman spectrum, a weak but significant peak in the range 152–166 cm^{-1} that can be tentatively assigned to the symmetric stretching vibration mode of the Se–I–Se three-body system. A weak but significant peak in the range 185–189 cm^{-1} is observed only in the FT-Raman spectrum of **2a**, **2b**, and **2d**; in our opinion it arises from the antisymmetric stretching vibration of the Se–I–Se group (antisymmetric stretching vibrations of slightly asymmetric Br_3^- and IBr_2^- three-body systems lead to a peak at about 190 cm^{-1} in the FT-Raman spectrum). In the case of **2a**, the higher intensity of this peak with respect to that at 159 cm^{-1} suggests a mixed origin for the former.

The FT-Raman spectrum of **3a** is dominated by two very intense peaks at 164 and 175 cm^{-1}; no other significant peaks are present in the spectrum. This compound also features $[(t\mathrm{Bu}_3\mathrm{PSe})_2\mathrm{I}]^+$ ions, charge balanced by "V-shaped" I_5^- anions that can be described as weak charge-transfer adducts $[I^-{\cdot}(I_2)_2]$. The two Raman peaks can therefore be assigned to the stretching vibrations of the two differently elongated diiodine moieties. Analogously, the FT-Raman spectrum of **4c** features a broad intense peak centered at 166 cm^{-1}, which can be assigned to the superimposed stretching vibrations of the various independent diiodine molecules present in the crystal structure. No other peaks are observed that could be assigned to the two crystallographically independent $t\mathrm{Bu}i\mathrm{Pr}_2\mathrm{PSeI–I}$ adducts present in the structure; this is in agreement with the ionic formulation $[t\mathrm{Bu}i\mathrm{Pr}_2\mathrm{PSeI}]^+\cdots\mathrm{I}^-$. The FT-Raman spectra of **5b** and **5d** are also dominated by peaks assignable to the stretching vibrations of the various diiodine molecules present in the two structures: the spectrum of **5b** features three peaks at 181, 172, and 167 cm^{-1}, whereas the spectrum of **5d** shows only one broad peak centered at 167 cm^{-1} with a shoulder at 180 cm^{-1}. These vibrations are in agreement with the structural features of the two compounds and underline the inability of FT-Raman spectroscopy to give detailed information on the structural features of polyiodides beyond the nature of their building blocks (I_2, I^-, and I_3^-).[16,25–30]

Conclusions

Trialkylphosphane selenides interact with various amounts of iodine giving Se→I bonds in adducts with the composition R_3PSeI_x (x = 2–7). The solid compounds exhibit a number of weak intermolecular "soft–soft" interactions (> 3 Å), namely, the expected variety of I···I interactions, but also Se···I interactions between cations and anions, and attractive Se···Se interactions between molecules and between cations. In general, these interactions in supramolecular networks can be rationalized in terms of unsymmetric 3c–4e systems and of n→σ* overlap. In solution, the complexes are kinetically labile with respect to rapid R_3PSe ligand exchange analogous to halogen-transfer reactions in systems R_3P/R_3PX_2 (X = Br, I) and R_3PSe/R_3PSeBr_2. Iodine coordination leads to significant downfield shifts in the ^{77}Se NMR signals. As in several other cases of donor–acceptor adducts with iodine, the molecular species R_3PSe–I–I are energetically close to the ionic species $(R_3PSe)_2I^+[I_3]^-$. Excess I_2 favors formation of R_3PSeI^+ cations that behave as soft electrophiles interacting with polyiodide anions.

Experimental Section

NMR spectra were recorded using Bruker spectrometers AC 200, Avance 400, and AMX 300, with 85% H_3PO_4, Me_2Se, and $SiMe_4$ as external or internal standards.

FT-Raman spectra, in the range 500–50 cm^{-1}, were recorded with a resolution of 2–4 cm^{-1} with a Bruker RFS100 FT-Raman spectrometer, fitted with an In-Ga-As detector (room temperature) operating with a Nd-YAG laser (excitation wavelength 1064 nm; 50–100 mW), with a 180° scattering geometry. The values in parentheses next to the reported wavenumbers represent the intensities of the peaks relative to the strongest peak, arbitrarily assigned the value 10.

Starting materials **1a**–**1d** were prepared according to published procedures;[31] all experiments were carried out in dry solvents under inert gas.

2a: A solution of iodine (0.762 g, 3.0 mmol) in dichloromethane (30 mL) was added slowly to a solution of *t*Bu$_3$PSe (**1a**) (0.843 g, 3.0 mmol) in dichloromethane (20 mL) in a Schlenk tube. The red–brown solution was stirred for a further 24 h at room temperature, after which the crude product **2a** was isolated by vacuum evaporation of the solvent and purified by washing with pentane and drying by vacuum evaporation. Crystallization by vapor diffusion from dichloromethane/pentane gave red–brown crystals. Yield: 1.46 g (91%). M.p. 113–114 °C. $C_{12}H_{27}I_2PSe$ (535.09): calcd. C 26.94, H 5.09, Se 14.76; found C 26.80, H 4.90, Se 14.60. EI-MS: *m*/*z* (%) = 408 (8) [(*t*Bu$_3$PSeI)$^+$], 281 (100) [(*t*Bu$_3$PSe)$^+$], 202 (7) [(*t*Bu$_3$P)$^+$]. FT-Raman (500–50 cm^{-1}): 86 (4.5), 115 (10), 123 (5), 159 (0.6), 189 (1) cm^{-1}. ^{31}P NMR (C_6D_6): δ = 83.1 (s, $^1J_{P,Se}$ = 579.9 Hz) ppm. ^{31}P NMR (CD_2Cl_2): δ = 83.6 (s, $^1J_{P,Se}$ = 576.4 Hz) ppm. ^{77}Se NMR (CD_2Cl_2): δ = 4.92 (d br., $^1J_{P,Se}$ = 564 Hz) ppm.

2b: The compound was synthesized according to the procedure described for **2a**, using 0.74 g of I_2 (2.92 mmol) in dichloromethane (30 mL) and 0.78 g of *t*Bu$_2$*i*PrPSe (**1b**) (2.92 mmol) in dichloromethane (20 mL). Crystallization by vapor diffusion from dichloromethane/pentane gave red–brown crystals. Yield: 1.18 g (77%). M.p. 146 °C. $C_{11}H_{25}I_2PSe$ (521.07): calcd. C 24.94, H 4.88; found C 25.36, H 4.84. MS (FAB, *o*-nitrobenzylamine matrix): pos., *m*/*z* (%) = 663 (2) [{(*t*Bu$_2$*i*PrPSe)$_2$I}$^+$], 395 (50) [(*t*Bu$_2$*i*PrPSeI)$^+$], 269 (78) [(*t*Bu$_2$*i*PrPSe)$^+$], 212 (38) [(*t*Bu*i*PrPSe)$^+$], 57 (68) [(*t*Bu)$^+$]; neg., *m*/*z* (%) = 432 (11) [(2 NBA + I)$^-$], 380 (12) [(I$_3$)$^-$], 280 (20) [(NBA + I)$^-$], 254 (5) [(I$_2$)$^-$]. EI-MS: *m*/*z* (%) = 268 (44) [(*t*Bu$_2$*i*PrPSe)$^+$], 254 (85) [(I$_2$)$^+$], 212 (28) [(*t*Bu*i*PrPSe)$^+$], 156 (54) [(*i*PrPSe)$^+$], 127 (10) [(I)$^+$], 57 (100) [(*t*Bu)$^+$], 43 (10) [(*i*Pr)$^+$]. FT-Raman (500–50 cm^{-1}): 111 (10), 166 (br., 1.5), 185.5 (0.3) cm^{-1}. ^{31}P NMR (C_6D_6): δ = 76.2 (s, $^1J_{P,Se}$ = 597 Hz) ppm. ^{31}P NMR (CD_2Cl_2): δ = 76.8 (s, $^1J_{P,Se}$ = 547 Hz) ppm.

2c: The compound was synthesized according to the procedure described for **2a**, using 0.762 g of I_2 (3.0 mmol) in dichloromethane (30 mL) and 0.759 g of *t*Bu*i*Pr$_2$PSe (**1b**) (3.0 mmol) in dichloromethane (20 mL). Crystallization by vapor diffusion from dichloromethane/pentane gave red–brown crystals. Yield: 1.3 g (85%). M.p. 126–128 °C. $C_{10}H_{23}I_2PSe$ (507.01): calcd. C 23.69, H 4.57; found C 23.88, H 4.61. MS (FAB, *o*-nitrobenzylamine matrix): pos., *m*/*z* (%) = 633 (5) [{(*t*Bu*i*Pr$_2$PSe)$_2$I}$^+$], 380 (58) [(*t*Bu*i*Pr$_2$PSeI)$^+$], 253 (86) [(*t*Bu*i*Pr$_2$PSe)$^+$], 57 (44) [(*t*Bu)$^+$]; neg., *m*/*z* (%) = 432 (8) [(2 NBA + I)$^-$], 380 (14) [(I$_3$)$^-$], 280 (46) [(NBA + I)$^-$], 254 (4) [(I$_2$)$^-$]. FT-Raman (500–50 cm^{-1}): 90 (0.4), 113 (10), 159 (0.4), 172 (0.3) cm^{-1}. ^{31}P NMR (C_6D_6): δ = 72.7 (s, $^1J_{P,Se}$ = 565 Hz) ppm. ^{31}P NMR (CD_2Cl_2): δ = 72.8 (s, $^1J_{P,Se}$ = 567 Hz) ppm. ^{77}Se NMR (CD_2Cl_2): δ = –61.25 (d, $^1J_{P,Se}$ = 565.7 Hz) ppm.

2d: The compound was synthesized according to the procedure described for **2a**, using 0.317 g of I_2 (1.25 mmol) in dichloromethane (20 mL) and 0.301 g of *i*Pr$_3$PSe (**1d**) (1.26 mmol) in dichloromethane (20 mL). Crystallization by vapor diffusion from dichloromethane/pentane gave red–orange crystals. Yield: 0.49 g (80%). M.p. 64 °C. $C_9H_{21}I_2PSe$ (493.01): calcd. C 21.93, H 4.29; found C 22.38, H 4.64. MS (FAB, *o*-nitrobenzylamine matrix): pos., *m*/*z* (%) = 607 (6) [{(*i*Pr$_3$PSe$_2$)I}$^+$], 367 (83) [(*i*Pr$_3$PSeI)$^+$], 241 (100) [(*i*Pr$_3$PSe)$^+$], 73 (73) [(*i*PrP)$^+$]; neg., *m*/*z* (%) = 433 (22) [(2 NBA + I)$^-$], 380 (35) [(I$_3$)$^-$], 280 (73) [(NBA + I)$^-$], 254 (17) [(I$_2$)$^-$], 127 (44) [(I)$^-$]. FT-Raman (500–50 cm^{-1}): 96 (0.7), 116 (10), 152 (0.9), 170 (0.2), 188 (0.2) cm^{-1}. ^{31}P NMR (CH_2Cl_2/C_6D_6): δ = 65.3 (s, $^1J_{P,Se}$ = 556 Hz) ppm.

3a: To a solution of *t*Bu$_3$PSe (**1a**) (0.560 g, 2.2 mmol) in toluene (30 mL) was added iodine (0.888 g, 3.5 mmol) in a Schlenk tube. The black precipitate that resulted after stirring for a further 24 h at room temperature was filtered off, dissolved in warm toluene solution, and cooled to –18 °C overnight. Green–black crystals of **3a** were isolated. Yield: 1.1 g (75%). M.p. 83 °C. $C_{12}H_{27}I_3PSe$ (661.99): calcd. C 21.24, H 3.97; found C 21.77, H 4.11. FT-Raman (500–50 cm^{-1}): 164 (10), 175 (4.2) cm^{-1}. ^{31}P NMR (CD_2Cl_2): δ = 82.9 (s, $^1J_{P,Se}$ = 565 Hz) ppm. ^{77}Se NMR (CD_2Cl_2): δ = 29.73 (d, $^1J_{P,Se}$ = 565 Hz) ppm.

4c: A solution of iodine (1.269 g, 5.0 mmol) in dichloromethane (20 mL) was added to a solution of *t*Bu*i*Pr$_2$PSe (**1c**) (0.506 g, 2.0 mmol) in dichloromethane (20 mL) in a Schlenk tube. The black precipitate that resulted after stirring for a further 24 h at room temperature was filtered off. After keeping the filtrate in dichloromethane for 3 d at room temperature under nitrogen gas, the solvent was partly evaporated and a crop of green–black crystals (**4c**, about 500 mg) could be collected from the dry part of the Schlenk tube. M.p. 108–109 °C. $C_{10}H_{23}I_4PSe$ (760.84): calcd. C 15.79, H 3.05; found C 13.21, H 2.48. FT-Raman (500–50 cm^{-1}): 111 (0.6), 166 (10) cm^{-1}. ^{31}P NMR (CD_2Cl_2 crystals): δ = 73.5 (s, $^1J_{P,Se}$ = 526 Hz) ppm. ^{31}P NMR (CD_2Cl_2 crystals): δ = 73.5 (s, $^1J_{P,Se}$ = 526 Hz) ppm. ^{77}Se NMR (CD_2Cl_2 crystals): no signals observed. ^{31}P NMR (CD_2Cl_2 solution with excess iodine): δ = 73.6 (d, $^1J_{P,Se}$ = 526 Hz) ppm. ^{77}Se NMR (CD_2Cl_2 solution with excess iodine): δ = 12.0 (d br., $^1J_{P,Se}$ = 539 Hz) ppm.

5b: A solution of iodine (2.71 g, 10.66 mmol) in dichloromethane (30 mL) was added to a solution of *t*Bu$_2$*i*PrPSe (**1b**) (0.570 g, 2.13 mmol) in dichloromethane (15 mL) in a Schlenk tube. After stirring at room temperature for 24 h, the black–green precipitate, crude product **5b**, was filtered off and washed with diethyl ether. Crystallization from dichloromethane gave green crystals of **5b**. Yield: 1.82 g (74 %). M.p. 75–85 °C. $C_{11}H_{25}I_7PSe$ (1155.59): calcd. C 11.43, H 2.18, I 76.87; found C 11.42, H 2.22, I 77.10. MS (FAB, *o*-nitrobenzylamine matrix): pos., *m/z* (%) = 663 (1) [{(*t*Bu$_2$*i*PrPSe)$_2$I}$^+$], 395 (69) [(*t*Bu$_2$*i*PrPSeI)$^+$], 269 (41) [(*t*Bu$_2$*i*PrPSe)$^+$], 212 (23) [(*t*Bu*i*PrPSe)$^+$], 57 (56) [(*t*Bu)$^+$]; neg., *m/z* (%) = 432 (7) [(2 NBA + I)$^-$], 280 (28) [(NBA + I)$^-$], 127 (30) [(I)$^-$]. EI-MS: *m/z* (%) = 268 (30) [(*t*Bu$_2$*i*PrPSe)$^+$], 254 (53) [(I$_2$)$^+$], 212 (19) [(*t*Bu*i*PrPSe)$^+$], 156 (38) [(*i*PrPSe)$^+$], 57 (100) [(*t*Bu)$^+$], 43 (10) [(*i*Pr)$^+$]. FT-Raman (500–50 cm^{-1}): 167 (10), 172 (9.8), 181 (3.7) cm^{-1}. ^{31}P NMR (CD_2Cl_2): δ = 76.5 (s, $^1J_{P,Se}$ = 528 Hz) ppm.

5d: A solution of iodine (0.862 g, 3.40 mmol) in dichloromethane (15 mL) was added slowly through a dropping funnel to a solution of *i*Pr$_3$PSe (**1d**) (0.198 g, 0.83 mmol) in dichloromethane (15 mL) in a Schlenk tube. The black–red solution was stirred for 4 h at room temperature, after which the crude product **5d** was isolated by vacuum evaporation of the solvent. Crystallization from dichloromethane gave red–brown crystals of **5d**. M.p. 60 °C. $C_9H_{21}I_7PSe$ (1127.15): calcd. C 9.59, H 1.88; found C 9.47, H 1.80. MS (FAB, *o*-nitrobenzylamine matrix): pos., *m/z* (%) = 675 (30) [(2 NBA + *i*Pr$_3$PSeI)$^+$], 607 (4) [{(*i*Pr$_3$PSe$_2$)I}$^+$], 367 (100) [(*i*Pr$_3$PSeI)$^+$], 241 (56) [(*i*Pr$_3$PSe)$^+$], 198 (16) [(*i*Pr$_2$PSe)$^+$], 73 (11) [(*i*PrP)$^+$]; neg., *m/z* (%) = 380 (41) [(I$_3$)$^-$], 280 (40) [(NBA + I)$^-$], 254 (24) [(I$_2$)$^-$], 127 (34) [(I)$^-$]. FT-Raman (500–50 cm^{-1}): 167 (10), 180 (sh., 4.6) cm^{-1}. ^{31}P NMR (CH_2Cl_2/C_6D_6): δ = 66.5 (s, $^1J_{P,Se}$ = 518 Hz) ppm.

Structure Determinations: Numerical details are presented in Table 5 and crystal data and structure refinement of complexes *t*Bu$_n$*i*Pr$_{3-n}$PSeI$_x$ are presented in Table 6. Data were recorded using monochromated Mo-K_α radiation at low temperature. Diffractometers used: Stoe STADI-4 (**2a**, **3a**), Bruker SMART 1000 CCD (**2b**, **2c**, **4c**, **5d**), and Siemens P4 (**2d**). Absorption corrections were based on ψ-scans for the point detectors and multiscans for the area detector. Structures were refined anisotropically on F^2 using the program SHELXL-97[32]. Hydrogen atoms were included using rigid idealized methyl groups allowed to rotate but not tip, or a riding model for other H atoms. In the Figures, ellipsoids are drawn to 50 % probability levels unless otherwise stated. For several structures, light atom displacement parameters were restrained (DELU, SIMU) to improve refinement stability. Special features/exceptions: structure **5d** was refined as a racemic twin; its methyl groups were refined riding and ideally staggered. Structure **3a** contains half a molecule of toluene (disordered over an inversion center) per formula unit; some butyl C atoms have high U values and their methyl groups were refined riding and ideally staggered. CCDC-239393 (**2a**), CCDC-686049 (**2b**), CCDC-686050 (**2c**), CCDC-686051 (**2d**), CCDC-116929 (**3a**), CCDC-686052 (**4c**), CCDC-116930 (**5b**), CCDC-116931 (**5d**) contain the supplementary crystallographic data (excluding structure factors) for this paper. These data can be obtained free of charge from The Cambridge Crystallographic Data Centre via www.ccdc.cam.ac.uk/data_request/cif.

Table 5. P–Se, (P)Se–I, (Se)I···I, Se···I, and Se···I distances [Å] in complexes $(R_3PSe)_x(I_2)_y$.

Compounds	*d*(P–Se)	*d*[(P)Se–I]	*d*[(Se)I···I]	*d*[(Se···I)]	*d*[(Se···Se)]
x/*y* = 1:1					
Ph$_3$PSeI$_2$ (I)	2.156	2.803	2.881	3.913	–
Ph$_3$PSeI$_2$ (II)	2.168	2.786	2.884	3.877	–
*t*Bu$_2$(*I*)PSeI$_2$	2.173	2.782	2.878	–	3.829
2a (I) ionic	2.194	2.765	–	4.057	–
2a (II) molecular	2.195	2.760	2.915	–	3.527
2b	2.205	2.783	–	3.880	–
2c (I)	2.181; 2.186	2.773; 2.779	–	3.996, 4.014	–
2c (II)	2.184; 2.186	2.776; 2.791	–	4.274; 4.319	3.435; 3.586
2d	2.190	2.777	–	3.864	–
(Et$_2$N)$_3$PSeI$_2$	2.203	2.715	2.985	4.293	–
(Me$_2$N)$_3$PSeI$_2$	2.178, 2.182	2.711, 2.721	2.960, 2.965	4.135, 4.250	–
x/*y* = 2:3					
3a	2.186, 2.190	2.737, 2.767	–	–	3.769
x/*y* = 1:2					
4c	2.212; 2.212	2.633; 2.620	3.129; 3.142	3.643; 4.195; 3.771, 4.060; 4.069	–
(Me$_2$N)$_3$PSeI$_4$	2.222	2.596	3.215	3.872	–
x/*y* = 2:5					
(Morph$_2$N)$_3$PSeI$_5$	2.214	2.590	3.186	3.644	–
x/*y* = 2:7					
5b	2.235; 2.237	2.563; 2.566	3.301; 3.248	3.644, 3.789	–
5d	2.208, 2.220, 2.226, 2.228	2.562, 2.563, 2.571, 2.578	3.266, 3.285, 3.286, 3.308	3.741, 3.792, 3.867; 4.000	–

Table 6. Crystal data and structure refinement of complexes $t\mathrm{Bu}_n i\mathrm{Pr}_{3-n}\mathrm{PSeI}_x$.

	2a	**2b**	**2c**	**2d**	**3a**	**4c**	**5b**	**5d**
Formula	$C_{48}H_{108}I_8P_4Se_4$	$C_{22}H_{50}I_4P_2Se_2$	$C_{20}H_{46}I_4P_2Se_2$	$C_{18}H_{42}I_4P_2Se_2$	$C_{27.5}H_{58}I_6P_2Se_2$	$C_{10}H_{23}I_4PSe$	$C_{22}H_{50}I_{14}P_2Se_2$	$C_{18}H_{42}I_{14}P_2Se_2$
M_r	2140.26	1042.08	1014.03	985.98	1370.00	760.81	2311.08	2254.98
Crystal size [mm]	0.70 × 0.50 × 0.40	0.35 × 0.14 × 0.14	0.22 × 0.14 × 0.10	0.75 × 0.70 × 0.65	0.75 × 0.50 × 0.50	0.30 × 0.25 × 0.20	0.23 × 0.22 × 0.19	0.44 × 0.16 × 0.05
Crystal system	triclinic	triclinic	monoclinic	triclinic	monoclinic	monoclinic	orthorhombic	orthorhombic
Space group	$P\bar{1}$	$P\bar{1}$	$P2_1/c$	$P\bar{1}$	$C2/c$	$P2_1/c$	$P2_12_12_1$	$Pna2_1$
a [Å]	8.694(2)	8.3441(8)	24.377(3)	8.1382(10)	31.687(5)	15.3098(14)	12.6693(10)	50.655(3)
b [Å]	14.874(4)	8.7208(11)	11.6720(12)	8.8174(10)	13.955(2)	12.3999(11)	16.4329(12)	15.5224(11)
c [Å]	15.141(4)	12.1373(12)	23.824(3)	11.3169(15)	19.383(2)	20.904(2)	25.2272(18)	12.5356(8)
α [°]	99.29(2)	84.250(3)	90	84.873(10)	90	90	90	90
β [°]	102.28(2)	69.941(3)	107.177(3)	69.654(10)	95.193(15)	95.238(3)	90	90
γ [°]	104.78(2)	89.485(3)	90	89.941(10)	90	90	90	90
V [Å^3]	1801.0(8)	825.14(15)	6476.2(13)	757.97(16)	8536(2)	3951.8(6)	5252.1(7)	9856.7(11)
Z	1	1	8	1	8	8	4	8
D_x [Mg m^{-3}]	1.973	2.097	2.080	2.160	2.132	2.558	2.923	3.039
μ [mm^{-1}]	5.582	6.089	6.203	6.622	6.164	8.213	9.714	10.348
transmissions	0.606–1.000	0.612–0.962	0.468–0.576	0.281–0.355	0.287–0.444	0.185–0.277	0.497–0.746	0.455–1.000
$F(000)$	1016	492	3808	460	5112	2752	4088	7920
T [K]	143(2)	143(2)	133(2)	173(2)	153(2)	133(2)	143(2)	143(2)
$2\theta_{max}$	55	61	56.56	50	50	61	60	56
reflections measured	12104	10179	117399	2803	13607	82382	43866	100493
reflections unique	8286	4979	16067	2657	7512	12063	15312	23779
R_{int}	0.0277	0.0335	0.0855	0.0115	0.0410	0.0338	0.0347	0.1086
no of parameters	311	148	533	128	358	303	378	650
no. of restraints	0	15	0	45	57	0	30	397
$R_w(F^2$, all reflections)	0.0722	0.0548	0.1261	0.0576	0.1388	0.0414	0.0380	0.1180
$R[F, I > 2\sigma(I)]$	0.0292	0.0251	0.0491	0.0237	0.0520	0.0209	0.0249	0.0585
S	1.17	0.98	1.06	0.99	1.15	1.05	0.89	0.95
max $\Delta\rho$ [e Å^{-3}]	1.42	0.97	2.97	0.71	1.19	1.04	1.74	3.12

---

[1] R. A. Zingaro, E. A. Meyers, *Inorg. Chem.* **1962**, *1*, 771–774.

[2] a) W. W. Schweikert, E. A. Meyers, *J. Phys. Chem.* **1968**, *72*, 1561–1565; b) M. Arca, F. A. Devillanova, A. Garau, F. Isaia, V. Lippolis, G. Verani, F. Demartin, *Z. Anorg. Allg. Chem.* **1998**, *624*, 745–749; c) D. C. Apperley, N. Bricklebank, S. L. Burns, D. E. Hibbs, *J. Chem. Soc., Dalton Trans.* **1998**, 1289–1292; d) M. Arca, F. Demartin, F. A. Devillanova, A. Garau, V. Lippolis, G. Verani, *J. Chem. Soc., Dalton Trans.* **1999**, 3069–3073.

[3] E. Krawczyk, A. Skowronska, *Phosphorus Sulfur Silicon Relat. Elem.* **1990**, *51/52*, 329.

[4] M. D. Rudd, S. V. Lindemann, S. Husebye, *Acta Chem. Scand.* **1997**, *51*, 689–708.

[5] S. M. Godfrey, S. L. Jackson, C. A. McAuliffe, R. G. Pritchard, *J. Chem. Soc., Dalton Trans.* **1997**, 4499–4502.

[6] a) W.-W. du Mont, *Main Group Chem. News* **1994**, *2*, 18; b) M. Bätcher, Ph. D. Thesis, University of Oldenburg, **1989**; c) J. Jeske, Ph. D. Thesis, Technical University of Braunschweig, **1997**.

[7] J. Jeske, W.-W. du Mont, P. G. Jones, *Chem. Eur. J.* **1999**, *5*, 385–389.

[8] D. J. Williams, K. J. Wynne, *Inorg. Chem.* **1976**, *15*, 1449–1451.

[9] (10-I-2): 10 valence electrons at the central iodine atom, which has 2 substituents. C. W. Perkins, J. C. Martin, A. J. Arduengo III, W. Lau, A. Alegria, J. K. Kochi, *J. Am. Chem. Soc.* **1980**, *102*, 7753–7759.

[10] S. M. Godfrey, S. L. Jackson, C. A. McAuliffe, R. G. Pritchard, *J. Chem. Soc., Dalton Trans.* **1998**, 4201–4204.

[11] C. G. Hrib, F. Ruthe, E. Seppälä, M. Bätcher, C. Druckenbrodt, C. Wismach, P. G. Jones, W.-W. du Mont, V. Lippolis, F. A. Devillanova, M. Bühl, *Eur. J. Inorg. Chem.* **2006**, 88–100; C. G. Hrib, F. Ruthe, E. Seppälä, M. Bätcher, C. Druckenbrodt, C. Wismach, P. G. Jones, W.-W. du Mont, V. Lippolis, F. A. Devillanova, M. Bühl, *Eur. J. Inorg. Chem.* **2007**, 4693.

[12] J. Konu, T. Chivers, *Dalton Trans.* **2006**, 3941–3946.

[13] W.-W. du Mont, A. Martens-von Salzen, F. Ruthe, E. Seppälä, G. Mugesh, F. A. Devillanova, V. Lippolis, N. Kuhn, *J. Organomet. Chem.* **2001**, *623*, 14–28; W.-W. du Mont, A. Martens-von Salzen, F. Ruthe, E. Seppälä, G. Mugesh, F. A. Devillanova, V. Lippolis, N. Kuhn, *J. Organomet. Chem.* **2001**, *628*, 280.

[14] a) S. Hauge, O. Vikane, *Acta Chem. Scand. Ser. A* **1983**, *37*, 723–728; b) W.-W. du Mont, H.-U. Meyer, S. Kubiniok, S. Pohl, W. Saak, *Chem. Ber.* **1992**, *125*, 761–766.

[15] E. Seppälä, F. Ruthe, W.-W. du Mont, P. G. Jones, *Chem. Commun.* **1999**, 1471–1472.

[16] C. G. Hrib, P. G. Jones, W.-W. du Mont, V. Lippolis, F. A. Devillanova, *Eur. J. Inorg. Chem.* **2006**, 1294–1302.

[17] C. G. Hrib, J. Jeske, P. G. Jones, W.-W. du Mont, *Dalton Trans.* **2007**, 3483–3485.

[18] W.-W. du Mont, F. Ruthe, *Coord. Chem. Rev.* **1999**, *189*, 101–133.

[19] a) W. A. S. Nandana, J. Passmore, P. S. White, *J. Chem. Soc., Chem. Commun.* **1983**, 526–528; b) F. Demartin, P. Deplano, F. A. Devillanova, F. Isaia, V. Lippolis, G. Verani, *Inorg. Chem.* **1993**, *32*, 3694–3699.

[20] P. G. Jones, C. Thöne, *Inorg. Chim. Acta* **1991**, *181*, 219–294.

[21] C. Daniliuc, C. Druckenbrodt, C. G. Hrib, A. Blaschette, P. G. Jones, W.-W. du Mont, *Chem. Commun.* **2007**, 2060–2062.

[22] V. Lippolis and F. Isaia in *Handbook of Chalcogen Chemistry*: *New Perspectives in Sulfur, Selenium and Tellurium*, Devillanova, F. A. (Ed.) **2006**, RSC Publishing, Cambridge, ISBN: 0–85404–366–7, ch. 8.2, pp. 477–499.

[23] P. D. Boyle, J. Christie, T. Dyer, S. M. Godfrey, I. R. Howson, C. McArthur, B. Omar, R. G. Pritchard, G. R. Williams, *J. Chem. Soc., Dalton Trans.* **2000**, 3106–3112.

[24] M. C. Aragoni, M. Arca, F. A. Devillanova, M. B. Hursthouse, S. L. Huth, F. Isaia, V. Lippolis, A. Mancini, *CrystEngComm* **2004**, *6*, 540–542.

[25] A. J. Blake, F. A. Devillanova, R. O. Gould, W.-S. Li, V. Lippolis, S. Parsons, C. Radek, M. Schröder, *Chem. Soc. Rev.* **1998**, *27*, 195–206.
[26] M. C. Aragoni, M. Arca, F. Demartin, F. A. Devillanova, A. Garau, F. Isaia, F. Lelj, V. Lippolis, G. Verani, *Chem. Eur. J.* **2001**, *7*, 3122–3133.
[27] M. C. Aragoni, M. Arca, A. J. Blake, F. A. Devillanova, W.-W. du Mont, A. Garau, F. Isaia, V. Lippolis, G. Verani, C. Wilson, *Angew. Chem.* **2001**, *113*, 4359–4362; *Angew. Chem. Int. Ed.* **2001**, *40*, 4229–4232.
[28] M. C. Aragoni, M. Arca, F. Demartin, F. A. Devillanova, A. Garau, F. Isaia, V. Lippolis, G. Verani, *Dalton Trans.* **2005**, 2252–2258.
[29] M. C. Aragoni, M. Arca, F. A. Devillanova, A. Garau, F. Isaia, V. Lippolis, A. Mancini, G. Verani, *Bioinorg. Chem. and Applications*, Vol. **2006**, Article ID 58937, pp 1–12, DOI 10.1155/BCA/2006/58937.
[30] M. C. Aragoni, M. Arca, F. A. Devillanova, A. Garau, F. Isaia, V. Lippolis, A. Mancini, *Bioinorg. Chem. and Applications*, Vol. **2007**, Article ID 17416, pp 1–46, DOI 10.1155/2007/17416.
[31] W.-W. du Mont, *Z. Naturforsch., Teil B* **1985**, *40*, 1453–1456.
[32] G. M. Sheldrick, SHELXL-97, *Program for Refinement of Crystal Structures*, University of Göttingen, Germany, **1997**.

Received: May 23, 2008